

UNCLASSIFIED

AD 272 062

*Reproduced
by the*

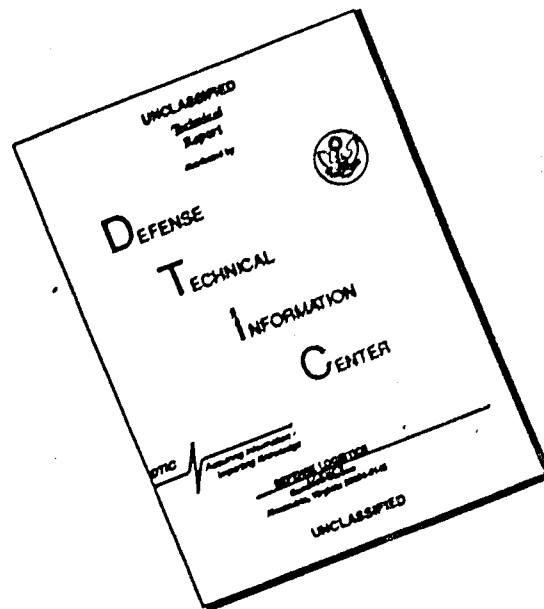
ARMED SERVICES TECHNICAL INFORMATION AGENCY
ARLINGTON HALL STATION
ARLINGTON 12, VIRGINIA



UNCLASSIFIED

NOTICE: When government or other drawings, specifications or other data are used for any purpose other than in connection with a definitely related government procurement operation, the U. S. Government thereby incurs no responsibility, nor any obligation whatsoever; and the fact that the Government may have formulated, furnished, or in any way supplied the said drawings, specifications, or other data is not to be regarded by implication or otherwise as in any manner licensing the holder or any other person or corporation, or conveying any rights or permission to manufacture, use or sell any patented invention that may in any way be related thereto.

DISCLAIMER NOTICE



THIS DOCUMENT IS BEST QUALITY AVAILABLE. THE COPY FURNISHED TO DTIC CONTAINED A SIGNIFICANT NUMBER OF PAGES WHICH DO NOT REPRODUCE LEGIBLY.

ASTIA

AS AD 100.

272002

272 062

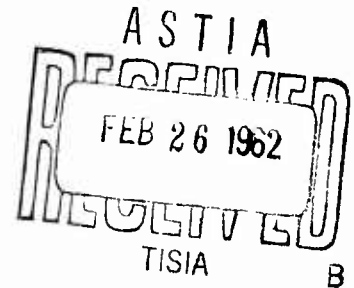
TWO-DIMENSIONAL MOTOR PROGRAM

P. D. Baker
R. G. Peoples
T. R. Mills

Aerojet-General Report
No. 2185
(Supplement to Report No. 2126)

JANUARY 1962

AEROJET-GENERAL CORPORATION
Azusa, California



NOX
2
2

22

TWO-DIMENSIONAL MOTOR PROGRAM

P. D. Baker
R. G. Peoples
T. R. Mills

Aerojet-General Report
No. 2185
(Supplement to Report No. 2126)

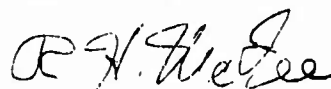
JANUARY 1962

AEROJET-GENERAL CORPORATION
Azusa, California

FOREWORD

This special report is a supplement to Aerojet-General Report No. 2126 (AFCSR 1802) and summarizes the work conducted on the Two-Dimensional Motor Program. This work was sponsored by the Air Force Office of Scientific Research on Contract AF 49(638)-178, Project No. 9751, Task No. 37510, and by Aerojet-General Corporation. The period covered is from December 1960 to December 1961.

Approved by:



R. H. McFee
Acting Manager
Advanced Research Division

ABSTRACT

A two-dimensional motor was designed, fabricated, and tested to establish improved techniques for measuring the dynamic characteristics of the combustion mechanism in an operating thrust chamber. The criteria on which the design of the motor was based, the experimental equipment, and the tests conducted are described. The methods by which this motor can be used to investigate stable and unstable combustion are discussed and the correlations necessary to relate the observed phenomena to the behavior of full-scale rocket engines are indicated.

TABLE OF CONTENTS

	<u>Page</u>
I. INTRODUCTION _____	1
II. DESIGN CRITERIA _____	2
A. Measurement of Available Energy _____	2
B. Transparent Motors _____	5
C. Operating Parameter Variations _____	10
D. Instrumentation _____	11
III. PARAMETER EVALUATION _____	13
A. Data Evaluation _____	13
B. Two-Dimensional Wall-Effect Correlation Factors _____	14
C. Full-Scale Evaluation _____	16
IV. DESCRIPTION OF THE PRESENT TWO-DIMENSIONAL MOTOR ASSEMBLY _____	17
A. Operating Conditions _____	17
B. Propellants _____	19
C. Equipment Description _____	20
D. Instrumentation _____	21
V. EXPERIMENTAL PROGRAM _____	23
A. Apparatus and Test Installation _____	23
B. Experimental Testing _____	24
C. Analysis and Interpretation of Experimental Data _____	26
VI. CONCLUDING REMARKS AND RECOMMENDATIONS _____	32
A. Conclusions _____	32
B. Recommendations _____	33
References _____	34

LIST OF ILLUSTRATIONS

	<u>Figure</u>
Typical Streak-Film Camera Arrangement _____	1
Typical Streak-Film Photograph _____	2
Derivation of Available Energy _____	3
Typical Particle Streak for a Constant-Velocity Recirculation Eddy ____	4
Elements of the Pulse Motor _____	5
Typical Measured Axial Velocity Contour for Two-Dimensional Flow _____	6a
Typical Measured Internal Velocity Contour for Two-Dimensional Flow ____	6b
Determination of Resultant Local Velocity for Two-Dimensional Flow ____	6c
Typical Resultant Velocity Contour for Two-Dimensional Flow _____	6d
Maximum Combustion Gas Velocity Profiles for Various Chamber Widths ____	7a
Maximum Combustion Gas Velocity Profiles for Various Chamber Lengths _	7b
Infinite-Wall Combustion Gas Velocity Profile _____	7c
Wall-Effect Correlation Curves for Various Width Chambers _____	7d
Chamber Assembly - Two-Dimensional _____	8
Injector - 3-in., Assembly of _____	9
Two-Dimensional Motor Test Installation, Test No. D-471-14-1 _____	10
Nozzle Assembly - Chamber _____	11
Insert-Oxidizer _____	12
Streak-Film Camera Locations _____	13
Two-Dimensional Motor Test Installation, Tests No. D-471-14-2-7 _____	14

LIST OF ILLUSTRATIONS (cont.)

	<u>Figure</u>
Explosion Damage, Test No. D-471-IM-1 _____	15
Typical Liner Erosion Pattern, Test No. D-471-IM-6 _____	16
Chamber-Pressure Record, Test No. D-471-IM-6 _____	17
Gaseous Particle Motion, Test No. D-471-IM-3 _____	18
Gaseous Particle Motion, Test No. D-471-IM-7 _____	19
Effect of Lucite Ablation on Combustion Efficiency _____	20
Detonation Waves, Test No. D-471-IM-1 _____	21
Combined Instability, Test No. D-471-IM-6 _____	22

	<u>Table</u>
Two-Dimensional Motor Tests and Experimental Results _____	1

LIST OF SYMBOLS

A, A_c	chamber cross-sectional area
A_t	throat cross-sectional area
a	acoustic velocity
C^*	characteristic exhaust velocity
c	unit heat of combustion
cps	cycles per second
d_o	orifice diameter
$\frac{dU}{dL}$	gaseous acceleration with respect to chamber length
f	frequency
ft/sec	feet per second
H	chamber height
L, L_c	chamber length
L^*	characteristic length
LN_2	liquid nitrogen
LO_2	liquid oxygen
l/d	orifice length-to-diameter ratio
M.R.	mixture ratio
m-sec	milliseconds
P_c	chamber pressure
psi	pounds per square inch
\dot{Q}	propellant burning rate
RP-1	rocket propellant (a hydrocarbon fuel)

LIST OF SYMBOLS (cont.)

T_c	chamber temperature
TPS	thrust-chamber pressure switch
t	time
t_s	time from fireswitch
\vec{U}_H	lateral velocity
\vec{U}_L	axial velocity
\vec{U}	resultant velocity
V_g	eddy recirculation velocity
V_j	injection velocity
W	chamber width
$\dot{w}_p, \dot{\omega}_p$	propellant flow rate
ϵ_a	pressure-sensitive energy available for release by a pressure perturbation
γ	ratio of specific heats
$\frac{\Delta L}{\Delta t}$	slope of a streak
ΔP_c	peak-to-peak amplitude of chamber pressure oscillation
η	combustion efficiency
τ	chemical combustion time
$\dot{\omega}_L$	window ablation rate

LIST OF SYMBOLS (cont.)

SUBSCRIPTS

$1, 2, 3, \dots$	order
(∞)	point at infinity
y	lateral
H.F.	high frequency
i	i th order
j	j th order
L	axial
L.F.	low frequency

I. INTRODUCTION

The ultimate goal of the investigators studying combustion instability is to establish sound criteria for the design of stably operating rocket engines.* Such design criteria, together with any resultant increase in the understanding of combustion, will form the basis of a technique for numerically predicting thrust-chamber performance. Analytical performance calculations based on a paper design and theoretical and/or empirical concepts will then be possible, reducing to a minimum the reliance on expensive "cut-and-try" experimental techniques.

The Two-Dimensional Motor Program discussed in this report is one approach to the achievement of this goal. The objectives of this program are (a) to establish a transparent-wall research device in which (b) the combustion mechanism could be quantitatively observed and (c) correlated to the phenomena as encountered in large-scale rocket engines.

Complete fulfillment of these objectives will result in both a significant advancement in rocket-engine design theory and an overall improvement in the basic understanding of the combustion process. Such information will aid in the eventual establishment of analytical techniques for predicting inherent stability.

A test and study program was initiated and completed which fulfilled the first two of the requirements listed above. The third objective of the Two-Dimensional Motor Program was beyond the scope of the work funded by the Air Force Office of Scientific Research under Contract AF 49(638)-178 and by Aerojet-General Corporation. The design, fabrication, and test installation, of the two-dimensional motor was accomplished on the AFOSR contract. The testing and report preparation were financed by Aerojet.

* As used in this report, "motor" means a research device and "engine" means a full-scale rocket engine.

Theoretical concepts were developed (Refs. 1 and 2) and qualitatively verified, using available experimental data previously developed on this contract (Ref. 3) which demonstrated that the inherent stability of a combustion process is primarily dependent on (a) the amount of pressure-sensitive energy available for release to a given pressure perturbation and (b) the relationship between the replenishment of this energy and the characteristics of the perturbation. Empirical equations relating the magnitude and distribution of pressure-sensitive energy in a combustor to engine operating parameters were developed. By using the two-dimensional motor for quantitative investigation of the combustion mechanism, it should be possible to refine the form of, and to evaluate the constants for, these empirical expressions. It will then be possible to establish the characteristics of pressure-sensitive energy within full-scale rocket engines.

The discussions contained in this report will detail (a) the design criteria, (b) the configuration, and (c) the testing of the two-dimensional motor. The significance of this device as a scientific research tool and recommended areas for future investigations will be discussed.

II. DESIGN CRITERIA

The objective of the two-dimensional motor was to provide a research device for the scientific determination of the parameters affecting and/or controlling the magnitude and spatial distribution of pressure-sensitive available energy in a full-scale combustion chamber.

The discussions below will describe the problems inherent in the measurement of available energy in a combustor and the criteria for designing a device for overcoming these difficulties.

A. MEASUREMENT OF AVAILABLE ENERGY

1. Available Energy Equation

The analytically derived relationships presented in Ref. 1 indicate that the pressure-sensitive energy available at any point in a combustion chamber can be expressed by the relationship

$$\epsilon_a = \frac{c\tau}{A} \frac{dU}{dL} \quad (1)$$

where

ϵ_a = pressure-sensitive energy available for release by a pressure perturbation

c = unit heat of combustion

τ = chemical combustion time

A = chamber cross-sectional area

$\frac{dU}{dL}$ = gaseous acceleration with respect to chamber length

A numerical value for the term $\frac{c\tau}{A}$ has not been accurately determined; for the purposes of this report it will be considered a constant. Based upon the limited qualitative data presently available, this assumption appears to be valid; consequently it is possible to determine a relative ϵ_a profile for a given combustor by measuring gaseous motion with respect to chamber length. Gaseous acceleration, $\frac{dU}{dL}$, and thus ϵ_a are determined by differentiating the absolute chamber-gas velocity profile with respect to length, at a series of points in the chamber.

2. Streak-Film Photography

Chamber-gas motion at any location within a combustion chamber can be determined using high speed, shutterless, "streak-film" cameras (Refs. 4, 5, 6, and 7). Cameras of this type have been used for many years to study combustion phenomena and have proved to be valuable research tools, once their limitations are recognized.

The camera is focused to view events within the combustion chamber through a transparent slit (see Figure 1). The film is exposed as it passes through the lens focal point at a high velocity, in a direction axially perpendicular to the camera lens and the transparent slit. The result of operating the camera in this manner, and without a shutter, is a film exposure similar to that in Figure 2. The dots along the edge of the film are millisecond timing marks used to determine the instantaneous film velocity and to time-correlate the data records.

The streaks recorded on the film are images of luminous gas particles in the moving gas stream. The slope of a streak, $\frac{\Delta L}{\Delta t}$, at a specified time and chamber location, represents the instantaneous local chamber-gas velocity component in the direction of the slit. If the slit is aligned in the direction of particle motion (i.e., along the axis of a streamtube), the particle acceleration (i.e., the rate of change of velocity with respect to distance) is obtained by differentiating the measured velocity profile with respect to chamber length. The necessary steps to derive a relative available energy profile are graphically illustrated in Figure 3.

For combustion chambers where recirculation eddies exist, it is virtually impossible to align a transparent slit in the direction of gaseous particle motion. Consequently accurate particle accelerations are exceedingly difficult to establish, as shown in the example below.

A hypothetical example of the streak that would be recorded for a recirculation eddy which lies in a plane parallel to the field of view of the camera is illustrated in Figure 4. Assume that the eddy has a constant recirculation velocity, V_g . If this streak were part of a film record being analyzed, and if it were not realized that an eddy existed, it is conceivable that an incorrect conclusion would be drawn regarding particle velocity. It might be concluded that particle velocity varies, at this point in time, from zero to V_g and back to zero again because the measured velocity is only that component of particle motion in the direction of the slit. Thus, when gaseous particle motion is composed of multi-directional components, the recorded velocity will be less than the actual velocity. The major problem in using streak-film photography to obtain velocity profiles is, therefore, the accurate determination of the absolute local chamber-gas velocity, U , where recirculation eddies exist.

Accurate velocity measurements can be made if the recirculation eddies can be eliminated so that the gas flow is parallel to the chamber axis, and if the streak-film slits can be aligned with the combustion-gas streamtubes. The limitation of this approach is that recirculation eddies do exist in full-scale combustion chambers. Hence, if they are eliminated in the research device,

it will be necessary to establish factors correlating the measured combustion gas-velocity profiles to those conditions where eddies do exist in full-scale chambers; this would be difficult.

If recirculation eddies cannot be eliminated, the combustion phenomena must be photographed in three orthogonal directions and the measured velocities vectorially summed to obtain a resultant velocity profile. The problems inherent in the development of a device capable of recording combustion-gas motion precisely in three dimensions at any point in the chamber are difficult or impossible.

One of the major criteria, therefore, for the design of any research device used for measuring available-energy profiles is to provide a means of controlling and distinguishing recirculation eddies whenever they exist. As will be shown later, this requirement can be fulfilled by using a test device which limits recirculation eddies to a single plane.

B. TRANSPARENT MOTORS

In formulating the design criteria for a transparent-walled rocket engine to be used on this program, a review was made of all available information on transparent-motor experiments (see Refs. 3 through 14 for a partial list). A brief description of the configuration, application, and limitations of several of these transparent motors, together with experimental data on them, is presented below.

1. The Pulse Motor

The purpose of the pulse motor (Figure 5) is to provide a research tool to simulate the operational characteristics of a full-size thrust chamber at moderate thrust levels, using durable, replaceable hardware. By incorporating within its design an instability-initiating mechanism, it is possible to control the onset of unstable combustion and to determine the relative susceptibility to instability of various engine-injector configurations. The characteristic behavior of an instability, during its initiation and growth, is determined by optical and mechanical observations. Detailed discussions of the pulse motor, its purpose, characteristics, uses, and resultant experimental data, are contained in Refs. 6, 8, and 9.

The pulse motor concept is basically sound, but it has several limitations that must be recognized. A discontinuous injection pattern deviating from the full-scale configuration is used (Figure 5) to make possible operation at moderate thrust levels. As a result, the propellant-mixing characteristics encountered with this type of injector differ significantly from those of the full-scale injector. Even though it is desirable that any research device used in studying combustion gas motion operate at these thrust levels, it can be concluded that the use of discrete injector pods cannot completely simulate full-scale engine conditions.

The cylindrical shape of the chambers of the pulse motor results in additional difficulties. It is difficult to define the location or characteristics of specific events in three-dimensional space where heterogeneous combustion is occurring. A cylindrical chamber does not lend itself to reducing or eliminating recirculation eddies, while under certain conditions (e.g., when discrete injector pods are used), it may actually promote eddies of undetermined strength. A more complete discussion of the problems encountered in using the pulse motor are discussed in Ref. 3.

2. The Wedge Motor

The wedge motor is a device designed to investigate experimentally the stable combustion mechanism. It was developed under another contract, and was used to extend the understanding of the combustion phenomena as studied under Contracts AF 18(600)-1155 and AF 49(638)-178. The wedge-motor design is based on the premise that, when a pie-shaped segment is removed from a full scale engine, the combustion process within that segment is not grossly altered. By placing walls along the radii of the segment, at least one of which serves as an observation window, it is possible to observe the full-scale thrust-chamber combustion mechanism, but at a more moderate thrust level. The design and operation of the wedge motor are discussed in Ref. 10.

It has been found that the wedge motor adequately simulates the full-scale combustion phenomena and yet allows the direct observation of its burning characteristics. Using this motor, it was possible to examine the injection characteristics more precisely than had previously been possible.

Comparison of the overall performance characteristics of the wedge motor to those of the full-scale engines indicated almost a one-to-one correlation. It should be noted that these comparisons were made at the exit-plane, with no attempt to determine variations in the actual combustion rate throughout the chamber. Moreover, no studies have been conducted to determine whether variations in the circumferential components of gas motion exist. It should be noted that the wedge motor was designed as a developmental tool; for this specific purpose, it has been quite satisfactory.

The wedge motor was used in conjunction with Contract AF 49(638)-173, to obtain the initial measurements of pressure-sensitive available energy. Streak-film photography was used to measure gaseous acceleration with respect to chamber length. By measuring the acceleration of the chamber gases, thus determining the relative rate of combustion products generation, it was possible to determine a relative available-energy profile for the motor. Initial measurements in the wedge motor did not consider motion in any direction other than the axial. However, these measurements did indicate the potential of this technique for evaluating available energy.

It should be noted that the measurements made in the wedge motor consisted of observing gaseous motion along a single fixed axial line. This line was not fixed with respect to the gaseous streamtubes within the chamber, because of their tendency to oscillate. Large velocity gradients between adjacent streamtubes were frequently observed. Thus, the oscillatory motion of the streamtubes causes an apparent velocity variation with respect to time at each axial point along the line of observation. Such variations in the recorded data indicate the necessity of determining the absolute velocity components at a number of points along each line of observation. This can only be done using orthogonal streak-film records, assuming that all gaseous motion exists in the two-dimensional plane of observation.

The simulation of full-scale combustion by the wedge motor is limited because of the shape of the chamber, which produces a very narrow combustion cross section at the thrust-chamber axis and thus restricts the events

occurring within this region. This motor also has the disadvantage of being strongly hardware-oriented, since the chamber walls and the injector are actually derived from operational rocket engines. It is therefore difficult, if not impossible, to modify the injector pattern or to control precisely the injection process. Also, there is no way in which the effects on the combustion process of the two side walls can be analyzed.

3. Two-Dimensional Motors

Two-dimensional transparent motors have been used by various investigators to study the combustion phenomena (Refs. 7, 12, and 13).

The device described in Ref. 7 was originally designed to investigate the combustion characteristics of a specific injector-thrust chamber combination. Later experimentation included the use of this engine as a research device to investigate various aspects of the combustion phenomena, such as reaction rates, mass and energy transfer, etc. Particular emphasis was put on the determination of velocity profiles by using streak-film photography. This device was also used to examine variations in the injection mechanism, together with resultant changes in combustion, during an instability.

Refs. 12 and 13 describe two different two-dimensional motors of approximately the same configuration, which were used to investigate variations in the combustion mechanism resulting from the use of several injector types. The first thrust chamber was a 100-lb thrust motor consisting basically of metal contour and injector plates clamped between two plastic sheets, which was designed to operate at a chamber pressure of 300 psia. The combustor had a uniform thickness of 1/2 in. and a characteristic chamber length (L^*) of approximately 60 in.

The second motor was a two-dimensional transparent thrust chamber approximating a slice, 0.47 in. thick, from a 1000-lb thrust rocket engine, which was also designed to operate at a chamber pressure of 300 psia. The combustor had a contraction ratio of 5.9 and an L^* of 57 in.

These motors had lucite windows affixed to both sides to permit observation of the combustion mechanism. The events occurring within the combustor were recorded by a framing camera at 3000 fr/sec. Flame-intensity fluctuations were recorded in the latter engine by a photoelectric cell.

Both motors were instrumented to measure steady-state and oscillatory chamber pressures. Low- and high-frequency instabilities were encountered and qualitatively measured in the former motor. The low-frequency unstable combustion oscillated at 100 cps, while the high-frequency instabilities oscillated at frequencies corresponding to the resonant characteristics of the chamber. It was found, in the latter motor, that the flame-intensity and pressure fluctuations were in phase.

Difficulties were encountered in the use of these motors because of window erosion and obstructed light transmission. The erosion was most severe at points of propellant impingement and at the nozzle throat. The plastic eroded at a rate equivalent to 20% of the propellant flow rate (Ref. 12) and resulted in an 8-14%/sec reduction in chamber pressure (Ref. 13). The transmitted combustion light became increasingly obscured during each test because of depositing of an opaque substance - probably carbon particles - on the inner window surfaces.

The information derived from these motors was very useful in establishing design criteria for the device used on this program. It was estimated, based on the testing of these motors and the wedge motor, that window erosion would not be a severe problem if direct liquid impingement was avoided. It was later determined (see Section V) that the plastic would erode without direct liquid impingement and surface burning if turbulent combustion occurred immediately adjacent to the liner.

One limitation common to all of these motors is that a method for determining the effect of the walls on the combustion process has not been established. Two-dimensional motor data cannot be used directly to describe the events within a full-scale engine because of (a) the differing effects of

the walls (e.g., heat transfer and frictional losses to the walls per unit volume of gas, channeling of the flow, etc.) and (b) the two-dimensional, rather than three-dimensional, flow characteristics. Therefore, if a two-dimensional motor is used, it is necessary to establish a technique whereby the observed two-dimensional data can be correlated to the full-scale combustion processes.

4. Summary

The shortcomings of the available combustion devices described above have precluded the precise, scientific evaluation of the combustion phenomena. In order to overcome the inherent difficulties encountered in these motors, a special device with transparent walls, the two-dimensional, variable-width motor, was selected as the best research tool for obtaining reasonably accurate velocity profiles.

A two-dimensional chamber will limit the gross gaseous motion to a single plane. This will reduce the required photography to the recording of events in two orthogonal directions and will eliminate many of the recirculation eddy problems inherent in such combustion devices as the wedge motor.

As mentioned above, the two-dimensional data cannot be used directly to describe the combustion phenomena in full-scale engines. Wall-effect correlation factors must first be derived and applied. A detailed discussion of the techniques used to establish these correlation factors is presented in Section III. It should be sufficient to state at this point that the technique involves experimentation in which the width of the combustor is varied.

C. OPERATING PARAMETER VARIATIONS

For a more realistic approach to the problem of determining the parameters affecting and/or controlling the magnitude and spatial distribution of pressure-sensitive energy, it is necessary that the configuration of the test device facilitate the control and variation of the operating parameters. Since the operating parameters must be variable, the major criteria for the hardware design are established as described below.

1. Chamber Pressure

It has been shown that the propellant burning rate is proportional to some power of the chamber pressure, and that the amount of energy available for release by a pressure perturbation, ξ_a , is related to the propellant burning rate, \dot{Q} (Ref. 1). Therefore it is necessary that this device be able to operate at pressures simulating those encountered in current full-scale engines in order that the effects of chamber pressure variations on ξ_a can be realistically studied.

Chamber pressure can be changed by varying either the propellant weight-flow density, \dot{w}_p/A_c , or the cross-sectional area of the throat, A_t . As will be seen later, it is desirable to be able to vary both of these parameters.

2. Injection Velocity

It has been shown in Ref. 15 that, as the propellant injection velocity increases, the propellant vaporization rate also increases. Since the propellant burning rate, \dot{Q} , is proportional to the vaporization rate and the available energy is, as mentioned above, related to \dot{Q} , it is necessary that injection velocity be variable so that its effects on ξ_a can be studied. The injection velocity can be varied either by keeping the injection orifice diameters, d_o , constant and varying the propellant weight flow density, \dot{w}_p/A_c , or by varying d_o while keeping \dot{w}_p/A_c constant. Again it would be desirable to be able to vary both.

3. Propellant Spatial Distribution

In the initial testing phase, it is necessary to use a homogeneous injection pattern, as discussed in Section III. Later in the program it will be necessary to study nonhomogeneous injection to achieve a more realistic simulation of the characteristics of full-scale injectors. From an economic standpoint, it would be advisable to minimize injector fabrication. This can be done by designing injectors whose configuration can be altered with a minimum amount of effort.

In order to investigate the effect of propellant spatial distribution on the magnitude and distribution of available energy, it is necessary for the injector to be designed so that its propellant injection characteristics can be controlled and precisely predicted.

4. Other Variable Parameters

The following parameters should also be variable:

- a. The propellant mixture ratio.
- b. The chamber width, in order to establish the wall-effect correlation factors previously mentioned.
- c. Chamber wall material. The ability to vary the composition of the material in the walls would make this motor a more flexible research tool. By using such variations, it would be possible to investigate the effects of varying heat sinks, material erosion, gas addition, etc.
- d. Chamber length, so that any particular engine configuration could be simulated more closely. The chamber should be at least long enough so that it operates efficiently under the most adverse propellant-mixing conditions.
- e. Propellant combinations. The motor should be capable of examining the combustion of the more common liquid propellants.

D. INSTRUMENTATION

1. Optical Techniques

The chamber should be designed so that several unobscured transparent slits, both parallel and perpendicular to the chamber axis, can be used simultaneously to view and record the combustion-gas motion with streak-film cameras.

Previous experience with streak-film photography has indicated that a high film velocity (e.g., 60 to 200 ft/sec.) is required to achieve an adequate degree of resolution. Superior photographic results may be derived if color film is used instead of black and white, since it has a greater latitude that may be useful in distinguishing events lacking in definition.

An accurate time-correlation between the film records and the other data records (e.g., oscillograph) is required. This is usually accomplished by placing 1000-cps timing marks on all records with a common occurrence mark appearing simultaneously at some point on each record. Timing marks are also needed in determining instantaneous film velocity in order to establish particle-velocity profiles.

The streak-film cameras must be oriented to permit an unobstructed view of the entire window slit, with minimum light diffraction.

It is also desirable, although not necessary, to photograph the gross combustion process, the propellant injection, and the ignition characteristics with a high-speed motion-picture camera such as the Fastex camera. These films should be taken in addition to any required documentary movies.

2. Mechanical Techniques

Chamber and manifold pressures must be measured with sufficient accuracy to provide a continuous record of both the mean pressure and any significant pressure oscillations. The latter measurements require the use of high-response sensing and recording devices.

Propellant flow rates must be measured with an accuracy corresponding to that of all other measurements. The more common flow-metering devices, rotating-vane meters and cavitating venturis, cannot be used to accurately determine instantaneous flow rates. Therefore, it is necessary to calibrate the injector so that instantaneous flow rates can be determined directly from the manifold temperatures and pressures and the chamber pressure.

Throat-pressure measurements, although not absolutely necessary, provide additional information (e.g., they indicate the magnitude of the ratio of specific heats for the combustion products) and aid in determining combustion efficiency.

To define the energy states throughout the combustor, it is necessary to measure chamber-gas temperature and pressure profiles and to correlate this information with the optically measured velocity profiles. The present state of the art in temperature- and pressure-sensing limits these measurements to the boundary layer.

III. PARAMETER EVALUATION

In order to evaluate the characteristics of the combustion phenomena as encountered in full-scale rocket engines, it is necessary to study and achieve a basic understanding of inherently simple combustion models. These studies are similar to the procedure required to understand the dynamics of real gas flow (i.e., it is necessary to study and understand non-viscous, incompressible flow before studying viscous, compressible flow). Therefore, it is necessary to establish the characteristics of the simpler two-dimensional combustion system before studying more complex problems.

A. DATA EVALUATION

1. Particle Motion

Two-dimensional chamber-gas motion can be recorded by high speed, shutterless, streak-film cameras. By recording the particle motion along several orthogonal transparent slits, two three-dimensional velocity contours are obtained for gas flow throughout the chamber in directions parallel and perpendicular to the chamber axis (Figure 6a and 6b). If these contours are vectorially summed (Figure 6c) a three-dimensional resultant velocity contour is obtained (Figure 6d). A three-dimensional relative available-energy contour can then be calculated by performing a three-dimensional vector differentiation on the velocity contour in Figure 6d (i.e., by plotting the maximum slope at each point of Figure 6d).

2. Chamber Gas State Points

The state of the chamber gases is established from the experimentally determined boundary-layer conditions (i.e., temperature and pressures), the three-dimensional velocity contour, and performance characteristics. A mean energy level as a function of chamber length is determined using the total measured thermal efficiency and the absolute-velocity profile. This energy distribution is used in conjunction with the transverse-velocity profile and the measured temperatures and pressures to establish an energy gradient. It is then relatively simple to divide the distributed energy into potential and kinetic components and to evaluate gaseous-state points (e.g., temperature, pressure, density, etc.).

B. TWO-DIMENSIONAL WALL-EFFECT CORRELATION FACTORS

The differences between two-dimensional and full-scale combustion can be partially accounted for by applying a wall-effect correction factor to the observed data. The applicability of these corrections is partially dependent upon the relative degree of one-dimensionality of the full-scale phenomena. The technique for establishing the required correction factors is to perform a series of tests on a variable-width chamber (1) by using a homogeneous injector pattern (i.e., one that will not cause recirculation eddies), (2) by varying the chamber width, and (3) by keeping all other engine parameters constant. The wall-effect correlation factors are then determined for each set of operating conditions by the method described below.

The maximum-velocity profile in the two-dimensional chamber (i.e., the profile down the center of the chamber) is determined and plotted for various chamber widths (Figure 7a). These curves are then cross plotted at various locations down the chamber. The result is a family of curves, similar to Figure 7b, each of which asymptotically approaches the full-scale (or infinitely spaced wall) chamber gas velocity for their respective axial locations. By plotting these asymptotic values vs chamber length (Figure 7c) a velocity profile, valid for the description of full-scale combustion with no recirculation, is obtained. By comparing each curve of Figure 7a with the curve in Figure 7c, two-dimensional wall-effect correlation curves (Figure 7d) are established for various chamber widths.

It is known that the maximum gaseous velocity within a channel has a tendency to be located along the passage centerline, and that the velocities recorded by streak-film photography are probably derived from observations made somewhat closer to the wall. It is therefore necessary, if accurate results are desired, to know both the velocity distribution across the chamber width and the depth of observation. With this information, it is possible to determine the infinite-wall velocity profile.

The depth of observation for current photographic techniques has not yet been established, but its resolution should be relatively straightforward. By analytically comparing the experimentally determined velocity profiles with engine performance (i.e., equating chamber-gas momentum as based on both velocity profiles and engine performance), it should be possible to establish the depth of observation and thus to develop the necessary correction factors.

The velocity distribution across the chamber width cannot be measured directly. It can be determined, however, by varying the chamber height and observing the effects of the end walls (i.e., the top and bottom of the chamber) on the velocity distribution vertically across the chamber at a given axial location. It is necessary to assume that the side walls (i.e., windows) affect the velocity profile across the chamber width, at that location, in the same manner as do the end walls. This is a valid assumption only if the materials of all four walls are the same and the injection pattern is symmetrical. These two considerations must be included in the design criteria for the two-dimensional engine if the maximum velocity profile is to be determined.

By following the above procedures during the initial testing of the two-dimensional motor, three sets of valuable and necessary information will be obtained: (1) wall-effect correlation curves for various engine operating conditions, (2) information on the behavior of homogeneous combustion, and (3) the region of observation within an operating chamber.

C. FULL-SCALE EVALUATION

Full-scale engine configurations can be evaluated either directly or indirectly using the two-dimensional motor.

1. Direct Full-Scale Evaluation

Engine operating characteristics are determined directly by examining various sections of the full-scale combustor in a two-dimensional motor and vectorially summing the experimentally measured velocity profiles. This approach is not so straightforward as it may appear, for it is dependent upon selection of each sector and its orientation. In order that the experimental results may be applicable as recorded or, at least, as determined following a minimum amount of numerical analysis, it is necessary that the sector matrix be made to include a large number of elements in which fluid flow is approximately one-dimensional. Sectors in which multidirectional gaseous motion is encountered are oriented in such a manner as to permit the examination of the more significant velocity components. (That is, the gaseous motion is restricted to two dimension, thus requiring that the plane of observation be located in the plane established by the major velocity components.) This technique permits the accurate determination of gaseous motion in all but a few elements, and in these remaining elements the results should be valid though not quantitatively accurate.

The examination of a combustor is divided into the determination of single and multidirectional flow characteristics as affected by the walls and as found far from any wall influence. The characteristics of each sector are vectorially summed and a three-dimensional contour describing the spatial distribution of available energy is established.

2. Indirect Full-Scale Evaluation

The indirect analysis of combustion performance requires little or no experimentation to evaluate each specific item of hardware. The entire analysis is based on numerical calculations made using experimentally determined

relationships, which describe the effect of each operating parameter, and the sources and sinks, on the spatial distribution of available energy. The configuration being investigated is divided into a matrix corresponding to the basic analytical elements and evaluated using a digital computer. The accuracy of these calculations is dependent on the validity of the empirical expressions and the combustion model. With sufficient prior experimentation, this numerical technique should permit quantitative examination of any full-scale engine combustion mechanism.

IV. DESCRIPTION OF THE PRESENT TWO-DIMENSIONAL MOTOR ASSEMBLY

A description of the transparent-walled two-dimensional motor which was fabricated and tested on this program (Ref. 3) is presented below (see Figures 8, 9, and 10).

A. OPERATING CONDITIONS

A brief survey of the operating characteristics of present-day rocket engines was made, since part of the design criteria for the two-dimensional motor called for simulation of the combustion behavior of these engines. From this survey it was determined that the following operating conditions would be representative and could be achieved using the two-dimensional engine:

Chamber pressure: $200 < P_c < 1000$ psia

Contraction ratio: $1.5 < \frac{A_c}{A_t} < 3.5$

Propellant weight-flow density: $0.5 < \frac{\dot{w}_p}{A_c} < 3.0$ lb/sec-in.²

Injection orifice diameter: $0.030 < d_o < 0.150$ in.

Propellant injection velocity: $20 < V_j < 200$ ft/sec

Chamber length: $6 < L_c < 22$ in.

Combustion efficiency: $90 < \eta < 100\%$

If empirical and/or analytical relationships are to be developed from the experimental data resulting from the use of this motor, it is imperative that the operating conditions be accurately defined and controlled. A brief discussion of the manner in which these operating conditions are controlled is presented below.

1. Control of Chamber Pressure:

Chamber pressure can be predicted for any given test by accurately controlling the propellant flow rates, mixture ratio, and contraction ratio. The state-of-the-art for testing medium-size thrust chambers limits propellant flow-rate control to $\pm 2\%$, mixture ratio to $\pm 4\%$, and contraction ratio to $\pm 2\%$. Therefore, chamber pressure can be predicted within $\pm 5\%$ for a given engine configuration, if the C^* efficiency is known. The chamber pressure can be measured within $\pm 3\%$.

2. Control of Injection Characteristics

The control of the propellant injection characteristics is important, since a deviation from the predicted propellant spatial distribution will alter the resultant chamber-gas velocity contour (Figure 6d). The propellant jets must therefore exhibit a high degree of directional and mass-flow stability.

Recommendations for the design of an orifice which will produce a stable, reproducible jet are found in Ref. 16. Such an orifice should have a long orifice-length-to-diameter ratio, l/d (i.e., an l/d of the order of 10 to 20), a contoured entrance, and a turbulence generator (i.e., a roughened section near the orifice entrance). It has been demonstrated (Ref. 16) that "turbulence-inducing devices tend to promote directional stability and reduce the effects of upstream disturbances." Not only will a long- l/d orifice improve jet directional stability but it will also tend to minimize the effect of chamber-pressure oscillations on the instantaneous propellant flow rate because of the relatively large drop in injection pressure. The resultant

stability tends to improve the homogeneous character of the combustion process and reduces the probability of incurring a low-frequency combustion instability.

To control propellant distribution in the combustion chamber, it is necessary that the static pressure be constant, or at least predictable, at the entrance to each injection orifice. A common problem encountered in many injectors is that of local manifold-pressure variations caused by high fluid-velocity gradients. These gradients result in nonuniform distributions of (a) static pressures within the manifold, (b) pressure gradients across each individual orifice, and (c) propellant within the chamber. Since these distribution functions are generally difficult to predict accurately, one of the design considerations for the injector is the reduction of the maximum manifold velocity to 10 ft/sec resulting in a velocity pressure head of less than 1.0 psi. As a result, it is possible to achieve a maximum variation of less than 1.0% in the injection velocity between similar orifices. This condition was satisfied in the fuel manifold, but not in the oxidizer manifold, because of the cryogenic properties of liquid oxygen (LO_2). A minimum LO_2 feed velocity is required to prevent significant vaporization of the liquid prior to injection into the chamber. In order to maintain this minimum velocity, no more than three oxidizer feed lines could be used. The resulting compromise oxidizer-feed configuration caused a 3% variation from the mean value of the injection velocity at the orifices in the immediate vicinity of the feed lines, for the tests with the highest flow-rate.

B. PROPELLANTS

The primary reason for selecting LO_2 /RP-1 as the propellant combination for the initial testing of this engine was that past experience had shown that good streak-film records are readily obtained with it. The burning of this propellant produces a high-temperature gas containing large amounts of luminous carbon particles which yield satisfactory streak-film records and are thus more readily photographable. Experience to date has shown that streak-film records

are difficult to obtain when nonhydrocarbon fuels such as N_2H_4 are used. This situation may possibly be improved by using fuel additives which do not otherwise affect combustion performance. Such techniques have not yet been proven but some experimentation has been done at Aerojet along this line with promising results.

C. EQUIPMENT DESCRIPTION

A description of the components used in the two-dimensional motor assembly is presented below.

1. Combustion Chamber

The maximum internal dimensions of the two-dimensional combustion chamber are 3.00 in. wide by 7.67 in. high by 22.0 in. long (Figure 8). All of these dimensions can be reduced to any size less than the maximum by using the proper size wall liners and nozzle inserts.

The chamber wall material can be varied. Wall liners of both lucite and zirconia-coated steel were fabricated and tested.

2. Nozzle

Three different throat-area nozzle assemblies were fabricated for a 1.00-in.-wide chamber and a single assembly for the 3.00-in. chamber. These nozzle assemblies have the following contraction ratios: 1.75, 2.46, and 3.46, and 2.46, respectively. Each nozzle has a rectangular cross section consisting of two flat and two contoured sections of refractory coated copper (Figure 11).

3. Injector

Two injectors having the same showerhead pattern were built, one for each type of chamber. The injection pattern (Figure 9) is symmetrical about a 45° angle with the chamber wall. The oxidizer and fuel orifices have

diameters of 0.055 and 0.052 in. and lengths of 1.50 and 0.50 in., respectively. They are equally spaced, 0.333 in. apart, in both directions. All orifices have a contoured entrance and a turbulence-inducing device as shown in the sketch of the oxidizer orifice in Figure 12. The distance between each wall and the nearest row of orifices is 0.167 in. The injector is designed so that the fuel-orifice plate can be removed and replaced by another plate with a different orifice configuration.

4. Windows

The design criteria for the transparent-walled motor stated that the window-clamping device should not obscure any part of the field of view of the streak-film camera. The load that each window was designed to carry is approximately 200,000 lb (i.e., 1000 psi over 200 sq in.), thus requiring a window thickness of approximately 4.0 in. to withstand these forces.

To avoid the expense of replacing these windows after each test, thin disposable liners were inserted between the flame and the window proper. This technique is fairly common where plastic is used both to contain the combustion process and to allow the experimental observation of the phenomena.

D. INSTRUMENTATION

1. Photographic Techniques

The majority of the significant data on this test program was to be recorded by streak-film photography. Four 35-mm General Radio Oscillograph Records were used to observe and record particle motion. Three were focused through axial transparent slits on one side of the chamber and the fourth was focused on a vertical slit on the other side (Figure 13). All four of these cameras had film speeds of about 80 ft/sec.

To obtain streak photographs for computing instantaneous local chamber-gas velocities, it is necessary to limit the camera's field of view to a narrow strip about 0.10 in. wide. This can be done by the following two methods: (a) A narrow slit is positioned near the focal plane of the

camera and perpendicular to the film edges in such a manner as to admit only the illumination from a narrow strip along the chamber wall; (b) the chamber walls are masked, so that only the illumination from a narrow slit is observed.

The first method has several disadvantages. If there is a relative vibration between the camera and the chamber, the section of the chamber viewed will vary with time and consequently instantaneous local velocities cannot be accurately determined. Also it is impossible to locate the mask exactly at the focal plane because this position is occupied by the film.

The advantages of the masked window approach are: (a) The chamber location viewed remains constant with time, and (b) when the proper safeguards are included, little extraneous chamber light strikes the film. It should be noted that this method cannot be used if more than one slit is being viewed on the same side of the motor, since it is possible that more than one slit would be in the field of view of each camera simultaneously. Therefore it is necessary to use a focal-plane mask in conjunction with the window slit. The focal-plane mask will eliminate all extraneous chamber light, while the window slit will restrict viewing to a specified location.

2. Pressure Measurement

A high-response pressure transducer (Photocon, Model 352) was mounted in the top of the chamber, 3.37 in. downstream from the injector face. The transducer could not be mounted flush because of the liner at this location. Therefore it was mounted 5/8 in. above the chamber inner face with a 1/8-in.-dia hole connecting the instrument and the chamber cavity.

Shock-tube tests indicated that the transducer, as mounted, has a flat frequency response in excess of 2500 cps.

Lower-response pressure transducers (Wankos) were connected to each of the injector propellant manifolds, to the chamber, and to the nozzle throat to record steady-state pressures.

V. EXPERIMENTAL PROGRAM

An experimental program to evaluate the operating characteristics of the two-dimensional motor was conducted. The installation and testing of the hardware, and the analysis of the resultant data are discussed below.

A. APPARATUS AND TEST INSTALLATION

For the first test of the series, the two-dimensional motor was installed as indicated in Figure 10. Cameras were mounted to view and record, through windows located on both sides of the engine, the events occurring within the thrust chamber. Three streak-film cameras (i.e., General Radio Oscillograph Recorders) were oriented to photograph particle motion in an axial direction while the other camera, on the opposite side of the engine, viewed particle motion in the transverse direction, (Figure 13). Framing cameras recorded the injection mechanism and the overall engine operating characteristics at 1000 and 64 frames per second respectively.

Following the initial test, it was determined that certain modifications in the test procedure and installation were required:

1. Additional igniters and a longer burning duration for the igniter
2. A shorter oxidizer-manifold pre-chill time
3. Smaller fuel and oxidizer internal-manifold volumes
4. An extended valve opening time
5. Additional blast protection for the cameras

The major changes to the test facility were the addition of a blast shield, the substitution of a steel window in place of the Lucite on one side of the chamber and the elimination of the transverse-motion recording camera. The test installation employed in all subsequent tests is shown in Figure 14.

A single igniter of 0.70-sec duration was installed in the top of the chamber on the first test. Three 4.0-sec igniters were installed on the chamber, one on the top and two on the bottom, for the second and third tests; three 2.2-sec igniters were used at the same locations for the final four tests.

It was found that the additional igniters provided the required igniter reliability on all tests after the first. The igniters were mounted outside the chamber and contained an Alclo-based, restricted solid grain.

$\text{LO}_2/\text{RP}-1$ was the propellant combination employed for this test series. In order to achieve a stabilized LO_2 temperature during injection into the combustor, the oxidizer manifold was pre-chilled prior to fire-switch, using LO_2 . The pre-chill time used on Test No. D-471-LM-1 was 5.0 sec.* Thereafter, it was found that the required amount of pre-chill could be satisfactorily accomplished by venting the cold oxygen vapor through the injector.

The start characteristics of the two-dimensional motor were modified by decreasing the volumes of the internal fuel and oxidizer manifold and increasing the propellant-valve opening time.

B. EXPERIMENTAL TESTING

The objective of the test program was to determine the validity of the two-dimensional motor as a research device. The scope of the program was not sufficiently broad to give a complete evaluation of the two-dimensional motor, but it was sufficient to indicate operating characteristics (see Section III). Because of limited time and funds, it was necessary to shorten the current program to a minimum number of firings. The test program as originally planned was to be conducted using two chamber widths - 1.0 and 3.0 inches - and two contraction ratios - 1.75 and 2.46. This program was to include investigations at three chamber pressures and three propellant flow rates. The mixture ratio, propellant combination, injection temperatures, wall material, etc., were to be held constant throughout the entire test program.

Damage to equipment during the first test necessitated the selection of an alternate scheme for parameter variation. The test conditions, as they were planned and conducted, are listed in Table 1.

A detonation occurred on the first test as the result of delayed ignition of propellant accumulated in the combustion chamber. The igniter flame

*Where tests are denoted as "Test No. X" it is to be understood that this means "Test No. D-471-LM-X."

had insufficient penetration to traverse from the top of the chamber to the bottom, where unburned propellant had accumulated during the start transient. The delayed ignition resulted in an explosion which damaged the four streak-film cameras, the injector assembly, and a set of Lucite windows. The damage resulting from this explosion is shown in the view of the test facility in Figure 15.

The test installation and experimental hardware were modified, as discussed above, to prevent further explosions. To determine the effectiveness of these modifications, an inert-propellant sequence test was conducted using liquid nitrogen, LN_2 , and RP-1. This test indicated that the major shortcomings in the test procedure had been eliminated.

Tests No. 3 and 4 were conducted with no major problems. The propellant flow rates on Test No. 3 deviated from the planned values because improper metering devices were used. The devices were corrected for Test No. 4.

An explosion occurred during Test No. 5, caused by a short in the igniter circuit and failure of the TPS (Time-Pressure Sensing) switch to properly terminate the test. The current to the igniters, at fire-switch, was insufficient to initiate igniter burning. The low chamber pressure due to non-ignition of the propellants should have been sensed by the TPS switch to terminate the test. However, because of the malfunction of the TPS switch, the propellants were continually injected and accumulated in the combustion chamber. A short in the sequence circuit applied an additional current impulse to the igniters shortly thereafter; this sufficed to initiate igniter burning, and the explosion resulted. (It should be noted that the total energy required to initiate igniter burning is approximately constant if applied over a short period. This energy could be applied by series of impulses, a single intense pulse, or a single extended low-level pulse of the same total-energy level.) Equipment damage in this explosion was limited to the loss of a Lucite window.

It should be noted that because of window ablation, the photographic data collected during these tests did not meet the minimum resolution required for accurate evaluations of particle motion. To improve both the performance of

the motor and the quality of the streak-film records, the area of Lucite in the liners exposed to the combustion flames was reduced. Zirconia-coated steel strips were used to replace the Lucite in all exposed locations except at the viewing slits. Tests No. 6 and 7 were conducted with the modified liners and an increase in performance was achieved. Even under these improved conditions it was found that there still existed sufficient ablation of the Lucite to cause severe attenuation and diffusion of the transmitted light.

Section II, above, discussed the basis for using plastic liners within the combustion chamber. The erosion encountered (see Figure 16) was greater than that found when using previous devices because of (1) the close proximity of propellant injection and combustion to the liners, and (2) the severity of the environmental conditions to which the Lucite was subjected. Previous motor configurations were designed with a definite separation between the viewing windows and the injected propellant jets, and consequently erosion was confined to areas of direct propellant impingement and to the nozzle throat. These motors generally operated at much higher contraction ratios, thus minimizing the effects of gas motion.

The data recorded during these tests is evaluated and its significance discussed below.

C. ANALYSIS AND INTERPRETATION OF EXPERIMENTAL DATA

As indicated in the preceding sections, the Two-Dimensional Motor Test Program has been hindered by difficulties in achieving the program objective. In spite of differences between the planned and actual operating conditions of the motor on these tests, valuable information was gathered which indicates the potential for this device.

1. Stable Operation

Any device which is designed to study the combustion mechanism as encountered in full-scale operational thrust chambers must simulate these conditions. It is impossible to examine a low-temperature, low-pressure Bunsen-burner flame and relate this information directly to realistic rocketry problems.

The experimental devices used in the analysis of combustion must duplicate combustor environmental conditions until sufficiently accurate analytical techniques are developed to eliminate the need for testing altogether. The approach taken years ago was simply to test and evaluate data from "work-horse" chambers similar in size and configuration to "flight" hardware. Considering the size and complexity of current engines, this is much more difficult. Furthermore, it becomes increasingly difficult to control scientifically all significant parameters.

The basis of the design criteria for the two-dimensional motor in achieving simulation of the configuration normally encountered in flight-type hardware was discussed in Section II. It is significant to note that unavoidable deviations exist between the combustor size and internal wetted perimeter of these devices. In order to qualify the two-dimensional motor as a valid research device, it is necessary to demonstrate that these differences can be reconciled. This can be accomplished by showing either that (a) variations in these parameters have little or no effect on the combustion mechanism, or that (b) it is possible to establish the necessary correlations to account for the deviations. One of the program objectives called for demonstrating the effect of chamber width on the gross combustion characteristics by conducting tests at two different chamber widths. The explosion which occurred on Test No. 1 destroyed an injector, thus limiting subsequent studies to a single width. The width employed on the remaining tests was 1.0 in., since it was felt that this configuration would subject the motor to a severer test of its capabilities.

a. Combustion Efficiency

Only one test, Test No. D-471-IM-6 (see Table I), achieved a combustion efficiency sufficiently high to be comparable to full-scale thrust chamber performance. Tests No. 3, 4, and 7 did not achieve adequate combustion efficiency because of off-mixture-ratio operation, excessive Lucite ablation, and chamber gas leakage, respectively. The lack of full-scale simulation on Tests No. 1, 2, and 5 is obvious; therefore, the analysis of combustion efficiency will be restricted to Test No. 6.

The chamber-pressure record for this test is shown in Figure 17. The instability shown on this figure will be discussed below. The motor achieved combustion efficiencies of 89.5% and 86.1% at times $t_s = 2.2$ and 2.4 sec. At $t_s = 2.2$ the igniters were still in operation; therefore the above efficiency has been corrected to account for the additional mass and energy. Had the efficiency been based solely on propellant flow rate and chamber pressure, it would have indicated an apparent efficiency of 93.6%. Contrary to the behavior exhibited throughout all other stages of the test, during this phase there was little evidence of unstable combustion, (see Figure 17). At $t_s = 2.4$ sec the thrust chamber had a low-frequency instability ($f = 76.6$ cps). This instability is discussed below. It should be noted that the chamber-pressure trace illustrated in this figure is an arithmetic mean.

These efficiencies are high, when chamber size is considered, and are only slightly lower than those encountered in flight hardware. Considering the effect of the low-frequency instability and the Lucite ablation, both of which result in a lower efficiency, the recorded performance is quite satisfactory.

b. Particle Motion

Figures 18 and 19 illustrate the recorded particle motion during the start transients of Tests No. 3 and 7. As discussed above, the ablation of the Lucite liners precluded the measurement of gaseous particle motion at any time other than during the initial stages of ignition. The curves shown are based on the gross motion of a series of luminous particles. As such they represent instantaneous motion along a streamline. Recirculation eddies are apparent in each of these figures. In Figure 18, combustion apparently occurs somewhere down-chamber, near the igniter, with the generated gases expanding toward both the injector and the nozzle. In Figure 19 gases are apparently being generated both at the injector and near the upper igniter. The resultant gas motion near the injector is toward the nozzle while gases generated near the igniter move toward both the injector and the nozzle.

Since mutually perpendicular slits were not used after the explosion on Test No. 1, it was not possible to determine the absolute gas velocity in the regions of recirculation. Hence it was not possible to derive velocity or available-energy profiles from the particle motions illustrated in these figures.

c. Window Ablation

Figure 16 shows the erosion caused by the chamber gases. This type of liner, with coated-steel strip inserts, was used on Tests No. 6 and 7. Solid Lucite liners without the strip inserts were used on all other tests. The significant point to note in this figure is the magnitude of the erosion and the amount of the carbon deposited.

The liner shown in Figure 16 has zirconia-coated steel inserts attached to the combustion side of the liner to minimize the amount of plastic exposed to the combustion gases. By reducing the total exposed Lucite surface area from 381 sq in. to 27 sq in. the time-average ablation rate was reduced from 1.5 lb/sec to 0.15 lb/sec (see Figure 20). The comparative change in combustion efficiency was from 70.2% to 86.1% for Tests No. 4 and 6 respectively (Table I). It is estimated that if no ablation had occurred the motor would have achieved a combustion efficiency of 88.3%.

2. Unstable Combustion

During the course of this test series, three distinct forms of unstable combustion were encountered. Instrumentation techniques employed on this program demonstrated its capability to accurately document each of these unstable modes.

a. Detonation Waves

Detonations within a thrust chamber are not particularly rare, but it is quite unusual to record anything other than the effects of a detonation wave on the test hardware.

The explosion which occurred on Test No. 1 was documented on streak film (Figure 21) as a record of the generation and propagation of a series of detonation waves. The initial detonation apparently developed near the igniter, forming two distinct fronts moving in opposite directions. The width of the wave-induced luminosity indicates that one front was reflected at the injector, overtook and coalesced with its counterpart. A second detonation wave appears at about the time that the first wave arrives at the nozzle entrance. The third wave recorded has the characteristics of a deflagration front because of its low front velocity. The maximum front velocities measured were 6320, 13400, and 3790 fps for the first, second, and third waves, respectively.

A typical luminosity trace which indicates gaseous-particle motion is shown in Figure 21. The particle velocities varied from 960 fps at the second wave to 1720 fps at the third wave.

The photographic records as indicated in Figure 21 are quite detailed. However, the pressure measurements yielded no data because of the extremely rapid sequence of events and time-response limitations of the transducers.

b. Low-Frequency Instability

Low-frequency unstable combustion was encountered during the starting transients of Tests No. 3, 4, and 6 and during steady-state operation of Test No. 6. This mode of unstable combustion is due to critical hydraulic coupling between disturbances in the chamber and the fuel manifold. The injection-pressure drop during these tests was never greater than 30 psi. Figure 17 illustrates the time history of the peak-to-peak amplitude of a low-frequency instability. The maximum peak-to-peak amplitude was 105 psi while the oscillation frequency remained approximately constant at 76.6 cps. The maximum peak-to-peak amplitude for the fuel-manifold pressure oscillation was 45 psi with a 62° phase shift between the chamber and fuel-manifold pressure oscillations. In Test No. 6, a low-frequency instability was not detected during steady-state chamber pressure operation, while the igniters were burning, or during the high-frequency instability.

c. High-Frequency Instability

Figure 17 shows the presence of high-frequency instability during the start transient of Test No. 6. The operating parameters that prevailed during the instability were:

Chamber pressure	$p_c = 152 \text{ psia}$
Propellant flow rate	$\dot{w}_p = 4.3 \text{ lbs/sec}$
Mixture ratio	M.R. = 1.8
Combustion efficiency	$\eta = 59\%$
Chamber temperature	$T_{c(\text{calc})} = 5450^\circ\text{R}$
Ratio of specific heats	$\gamma_{(\text{calc})} = 1.145$
Acoustic velocity	$a = 3940 \text{ fps}$

The instability had an average peak-to-peak pressure amplitude of 70 psi and a frequency of 2650 cps. The streak-film photographs indicated that the instability was moving in a transverse direction. (The resolution of the event on the film was satisfactory for viewing but was not sufficient for reproduction.) The values as reported have a tolerance of as much as $\pm 10\%$ because of the transient conditions and instrumentation response. Therefore, though an accurate analytical correlation could not be made, it can be concluded that the recorded instability was a transverse mode. Furthermore, it is probable that the transverse high-frequency instability was triggered by the low-frequency instability.

A different form of high-frequency unstable combustion occurred on Test No. 6, simultaneously with that of a low-frequency instability as shown in Figure 22. The high-frequency and low-frequency instabilities were superimposed in such a way that when the low-frequency amplitude was at its minimum value the high-frequency amplitude was at its maximum value. The maximum measured peak-to-peak amplitude was 25 psi, and the frequency of oscillation was 2300 cps.

VI. CONCLUDING REMARKS AND RECOMMENDATIONS

A. CONCLUSIONS

On the basis of the experimental program described in this report, the following remarks can be made regarding the utility of the two-dimensional motor as a combustion research device. These remarks summarize the findings of the first two phases of the Two-Dimensional Motor Program. These studies did not, nor were they expected to, provide all of the information necessary to describe the operating characteristics of the two-dimensional motor or the mechanism determining inherent stability. It will be the purpose of future studies to complete the requirements of the overall program.

1. It is possible to achieve the degree of optical resolution, in viewing events within the two-dimensional motor, required for the accurate determination of combustion characteristics.

2. By accurately measuring the spatial distribution of kinetic energy and the gaseous boundary layer temperature and pressure distributions, it should be possible to define the total energy state within the combustor.

3. Many of the characteristics of unstable combustion can be studied using the two-dimensional motor. Such investigations can even include the experimental observation of the detonation phenomena.

4. The effects of material erosion, of the physical and chemical properties of the propellant-injector design, etc., can be evaluated to determine their influence on the characteristics of the combustion mechanism. Knowing the relationship between the injector design and the combustion mechanism, it is possible to evaluate the effect of injector design variations on such considerations as the erosion of materials in the combustor.

5. It is possible to record experimental data with the precision required to establish the necessary empirical relationships for describing combustion.

It should be noted that these remarks are based upon the validity of the techniques described in Sections II and III.

B. RECOMMENDATIONS

The discussions in Section V and above indicate that the two-dimensional motor is a useful device and can be used to advance the state of the art in combustion research. However, to achieve its full potential, certain basic modifications must be made in the present design, including the following:

1. The use of optical-quality quartz in all viewing slits to minimize ablation of window material.
2. The use of several mutually perpendicular slit-windows to evaluate the dimensional velocity contours.
3. The use of boundary-layer temperature- and pressure-sensing devices to establish energy state points.

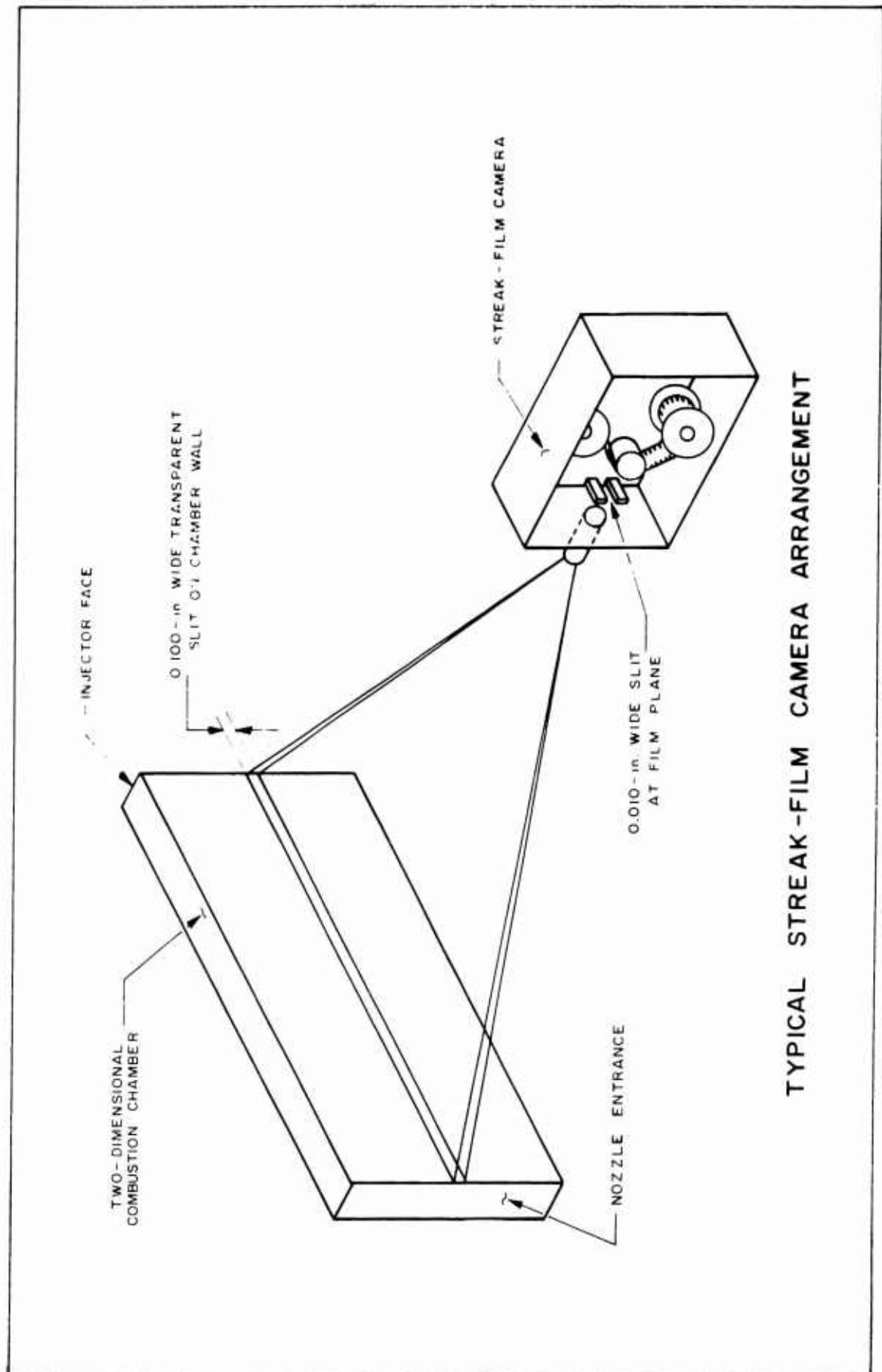
By incorporating these modifications into the basic hardware and conducting a complete test series, in which the effects of all significant variables (e.g., chamber pressure, mixture ratio, injector design, chamber configuration, etc.) are investigated, it should be possible to establish relationships between these parameters and the combustion mechanism. It will then be relatively simple to determine a relationship between any operating parameter and inherent stability and to establish the technique for predicting full-scale engine performance.

REFERENCES

1. R. S. Pickford and R. G. Peoples, Inherent Stability of the Combustion Process, Aerojet-General TN-36 (AFOSR 676), November 1960.
2. R. G. Peoples and R. S. Pickford, Analytical and Experimental Scaling of Thrust Chambers, Aerojet-General TN-40 (AFOSR 677), November 1960.
3. R. G. Peoples, P. D. Baker, and L. S. Knowles, High-Frequency Combustion Instability, Aerojet-General Report No. 2126, (AFOSR 1802), November 1961.
4. K. Berman and S. H. Cheney, "Combustion Studies in Rocket Motors," Journal of the American Rocket Society, 23, 2, March-April 1953.
5. T. Male, W. R. Kerslake, and A. O. Tischler, Photographic Study of Rotary Screaming and Other Oscillations in a Rocket Engine, NACA RM E54A29, May 25, 1954.
6. P. D. Gray and H. C. Krieg, Pulse-Motor Evaluation of Injector-Pattern Combustion Stability with Storable Propellants, Aerojet-General Report 1664, 29 July 1960 (Confidential).
7. S. Iambiris and L. P. Combs, Steady-State Combustion Measurements in a LOX/RP-1 Rocket Chamber and Related Spray Burning Analysis, Rocketdyne Research Report 61-13, 10 May 1961.
8. H. B. Ellis and R. S. Pickford, High-Frequency Combustion Instability, Aerojet-General TN-17 (AFOSR-TN-56-547), September 1956.
9. R. S. Pickford, H. C. Krieg, and H. B. Ellis, Basic Research in Liquid Rocket Thrust Chambers, Aerojet-General Report 1193 (AFOSR-TR-56-61), January 1957.
10. H. C. Krieg, L. O. Schulte, and P. D. Gray, Liquid-Thrust-Chamber Development Tools, Aerojet-General Report 1858, August 1960 (Confidential).
11. K. Berman and S. E. Logan, "Combustion Studies with a Rocket Motor Having a Full-Length Observation Window," Journal of the American Rocket Society, 22, 2, March-April 1952.
12. D. R. Bellman, J. C. Humphrey, and T. Male, Photographic Investigation of Combustion in a Two-Dimensional Transparent Rocket Engine, NACA Report 1134, 1953.
13. J. H. Altseimer, "Photographic Techniques Applied to Combustion Studies - Two-Dimensional Transparent Thrust Chambers," Journal of the American Rocket Society, 22, 2, March-April 1952.

REFERENCES (Cont.)

14. M. F. Heidmann and C. M. Auble, Injection Principles from Combustion Studies in a 200-Pound-Thrust Rocket Engine Using Liquid Oxygen and Heptane, NACA RM E55C22, June 7, 1955.
15. R. J. Priem and M. F. Heidmann, Propellant Vaporization as a Design Criterion for Rocket-Engine Combustion Chambers, NASA TR R-67, 1960.
16. J. H. Rupe, The Liquid Phase Mixing of a Pair of Impinging Streams, JPL Progress Report 20-195, August 6, 1953.



TYPICAL STREAK-FILM CAMERA ARRANGEMENT

Figure 1

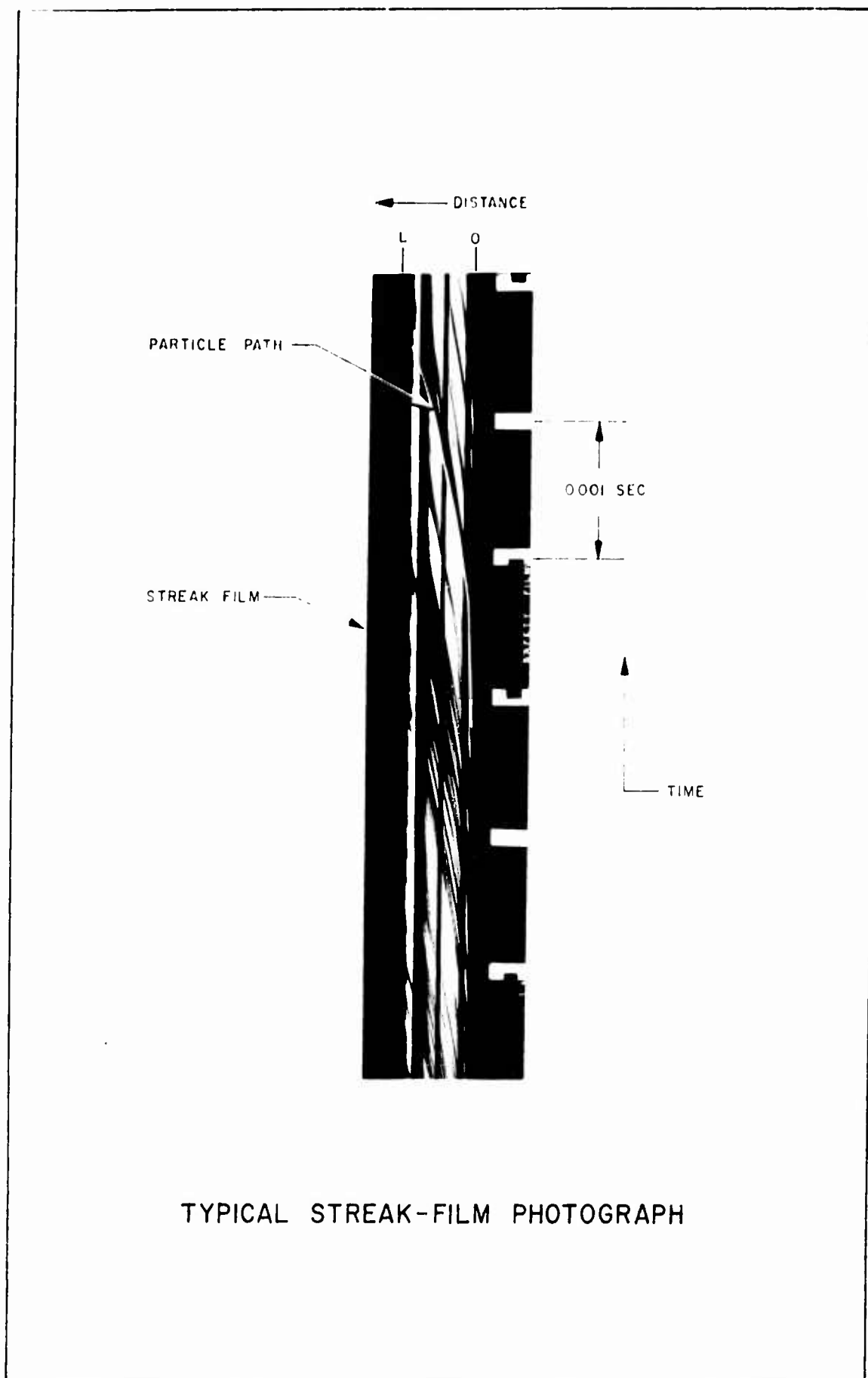
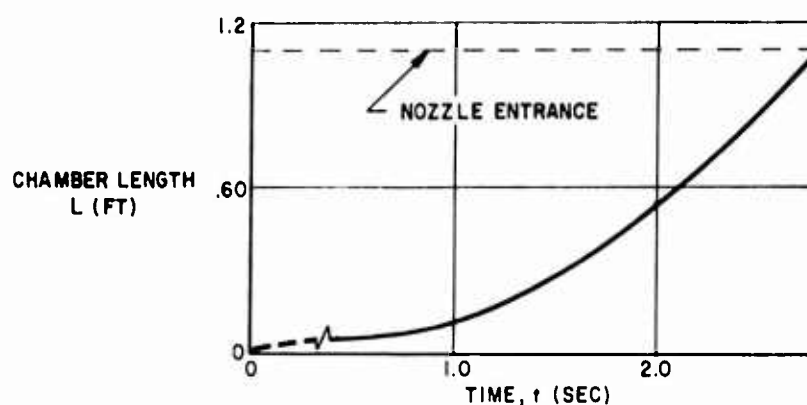
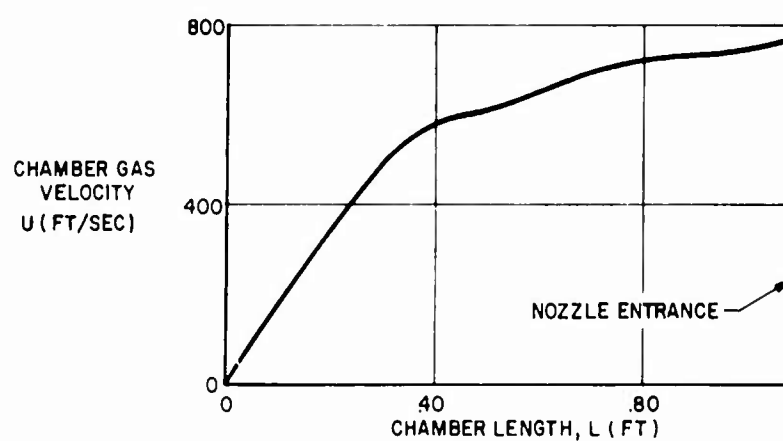


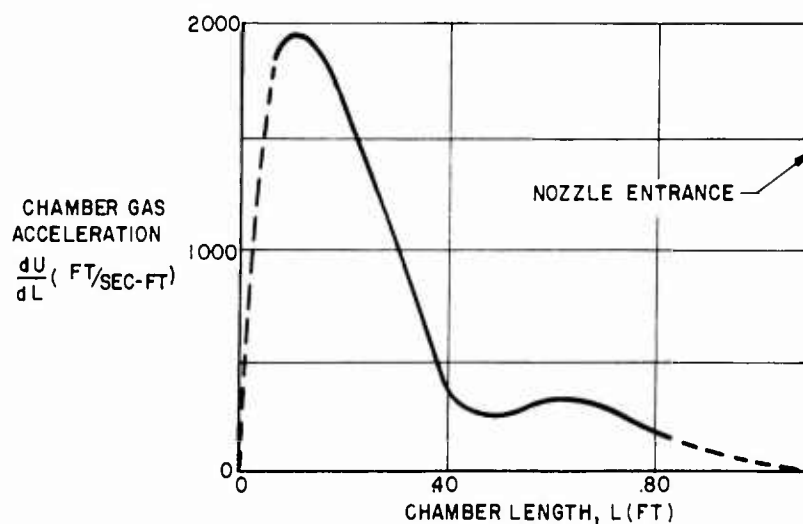
Figure 2



a. TIME WISE PLOT OF PARTICLE PATH



b. GAS VELOCITY ALONG CHAMBER



c. CHAMBER GAS ACCELERATION ALONG CHAMBER

DERIVATION OF AVAILABLE ENERGY

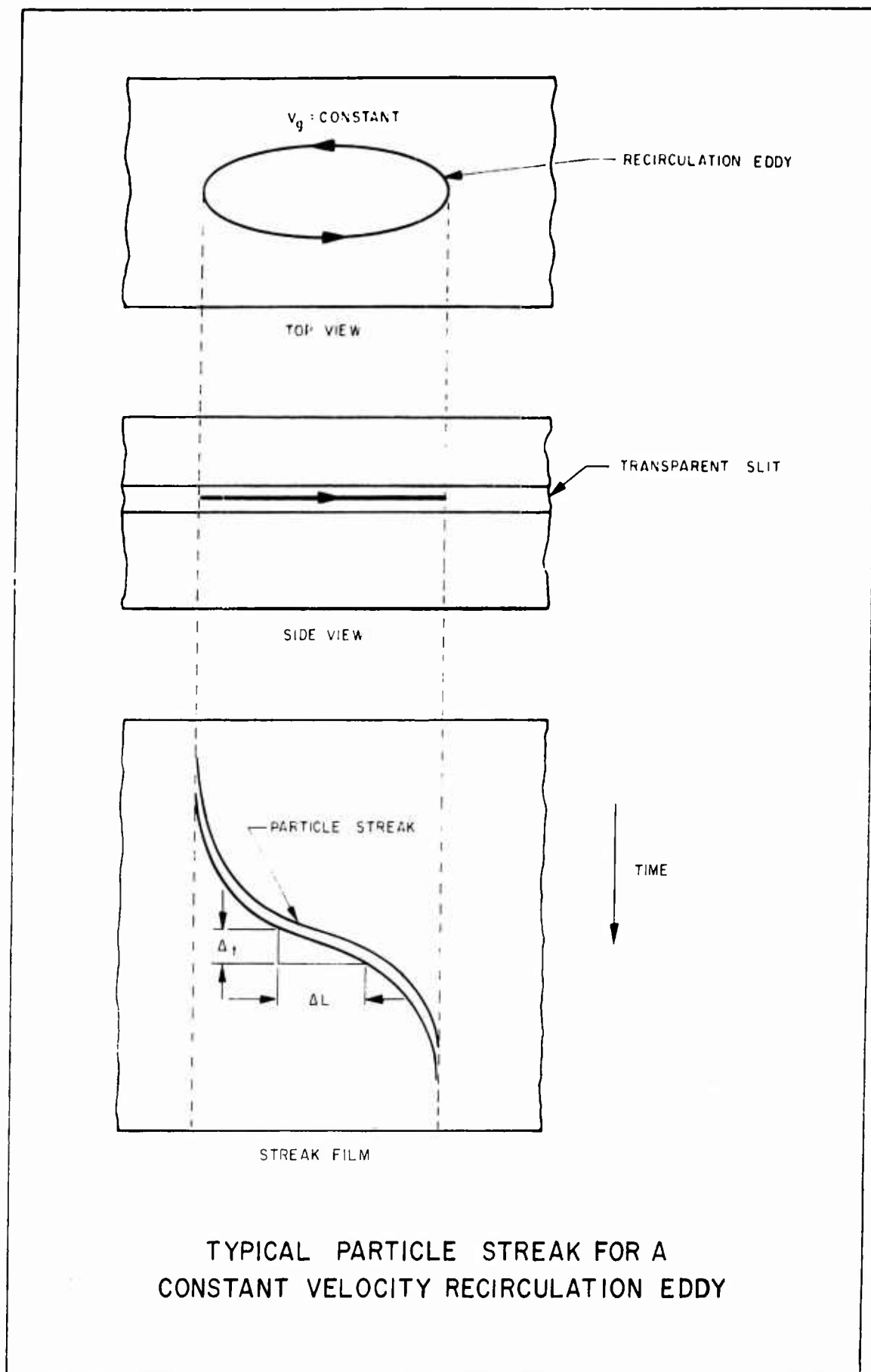


Figure 4

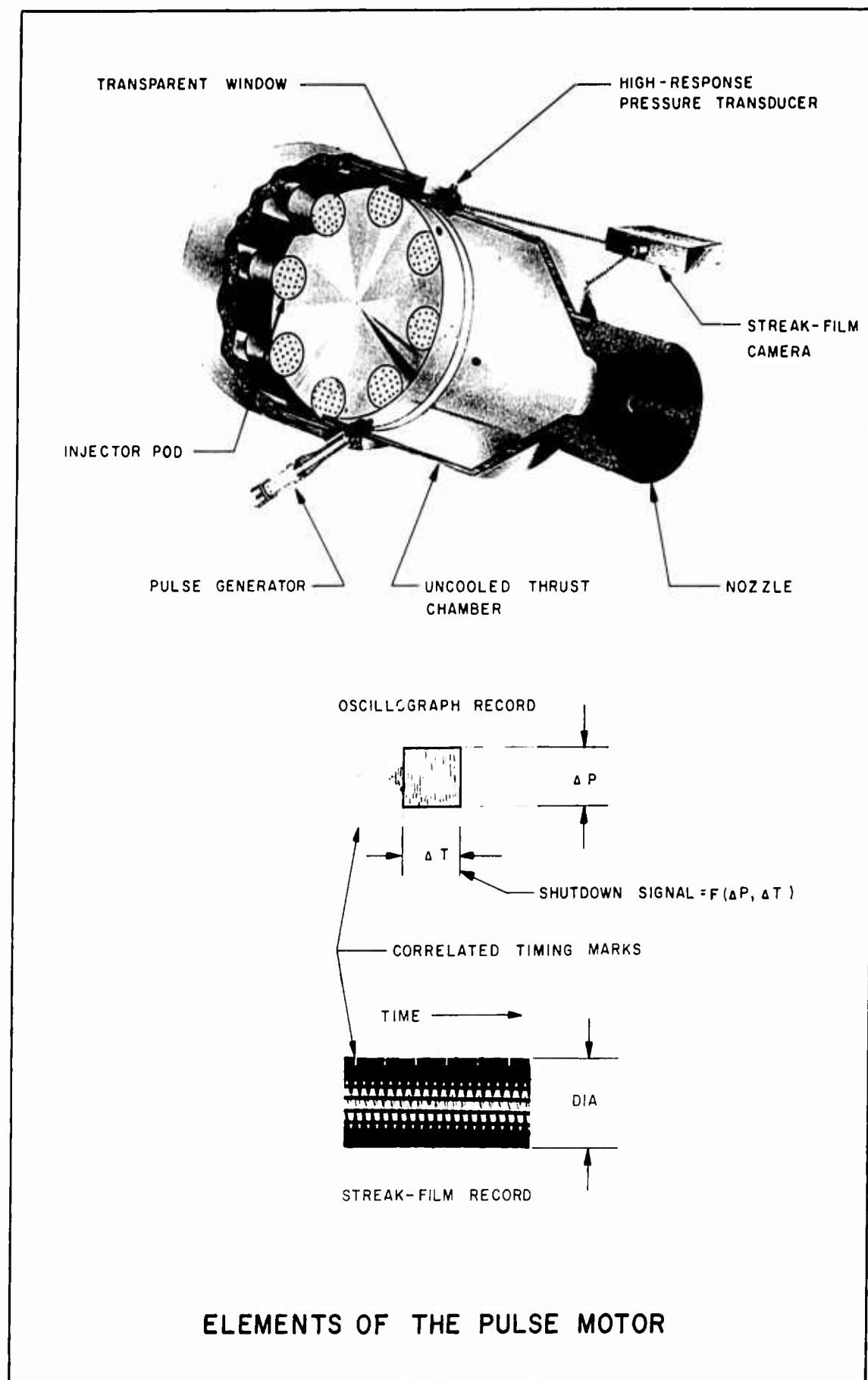
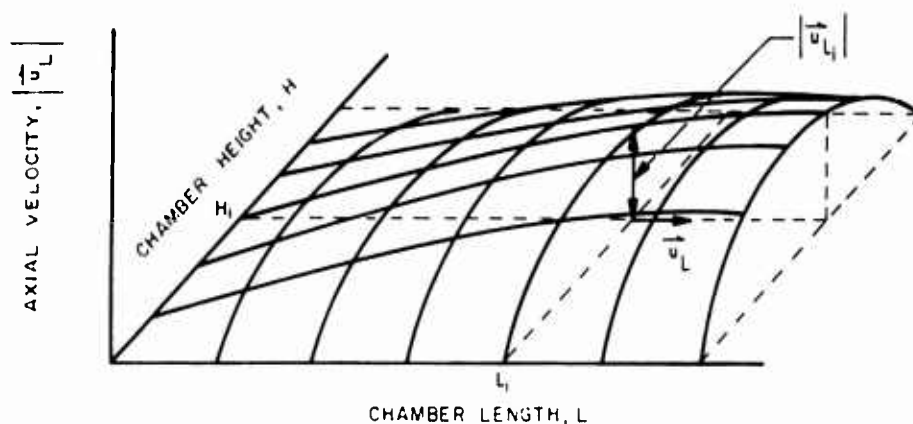
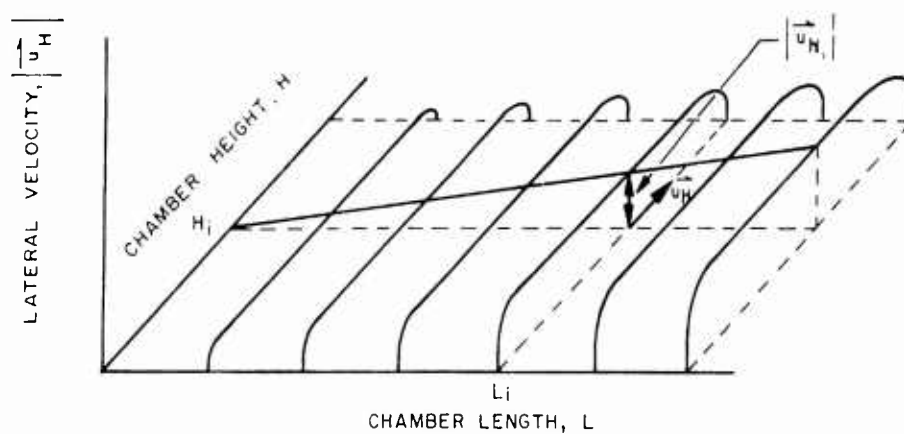


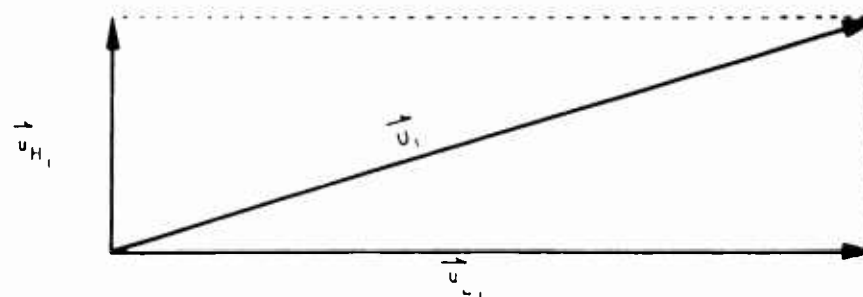
Figure 5



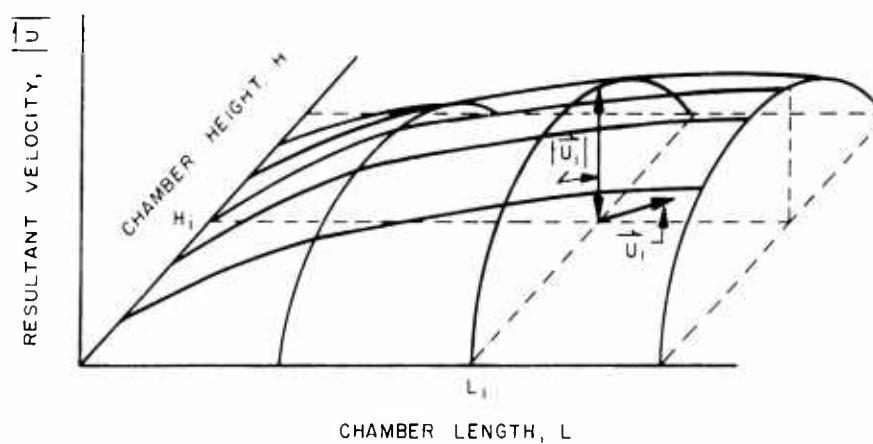
a. TYPICAL MEASURED AXIAL VELOCITY
CONTOUR FOR TWO-DIMENSIONAL FLOW



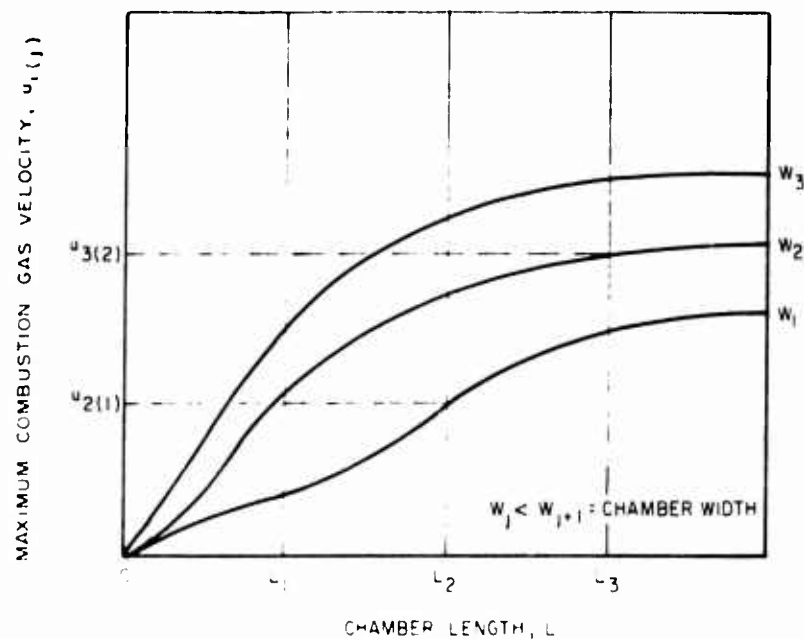
b. TYPICAL MEASURED LATERAL VELOCITY
CONTOUR FOR TWO-DIMENSIONAL FLOW



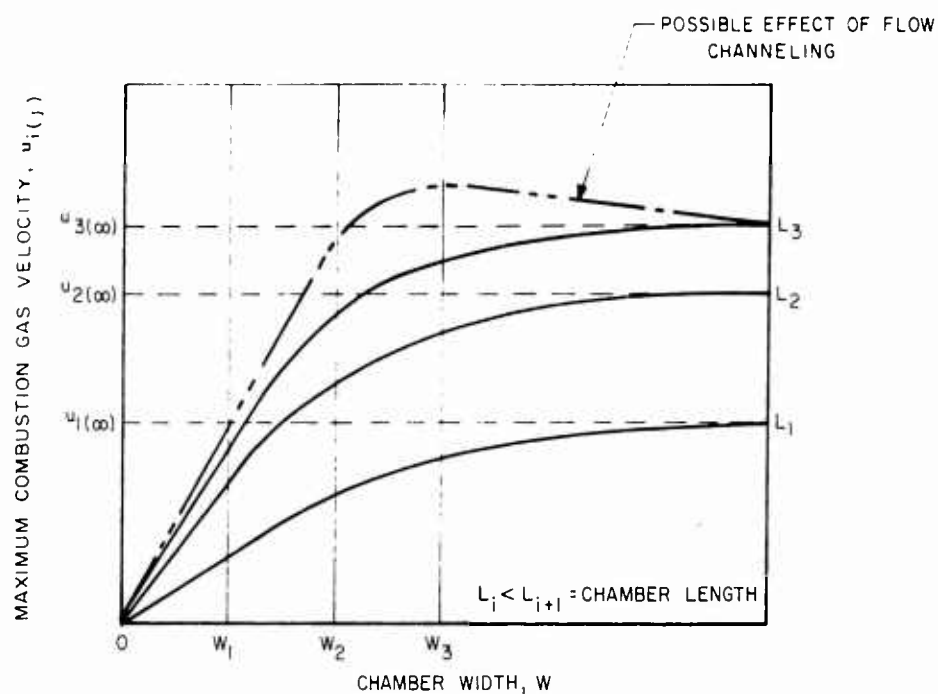
c. DETERMINATION OF RESULTANT LOCAL VELOCITY FOR TWO-DIMENSIONAL FLOW



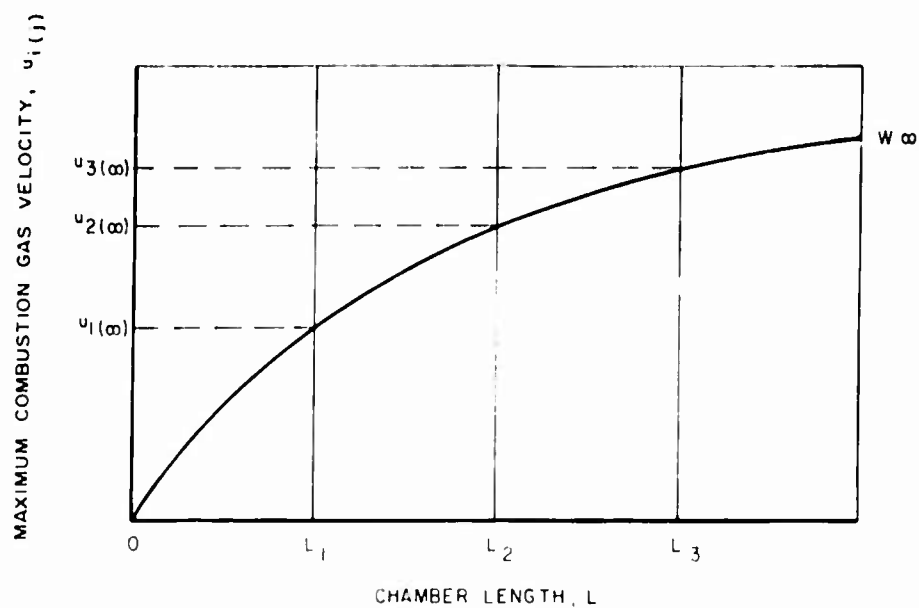
d. TYPICAL RESULTANT VELOCITY CONTOUR FOR TWO-DIMENSIONAL FLOW



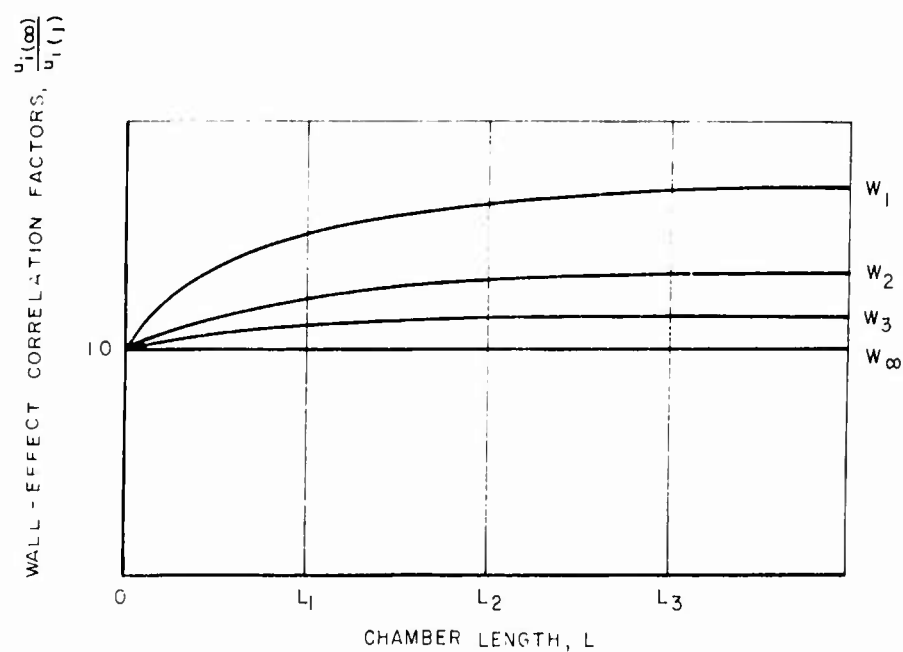
a. MAXIMUM COMBUSTION GAS VELOCITY
PROFILES FOR VARIOUS CHAMBER WIDTHS



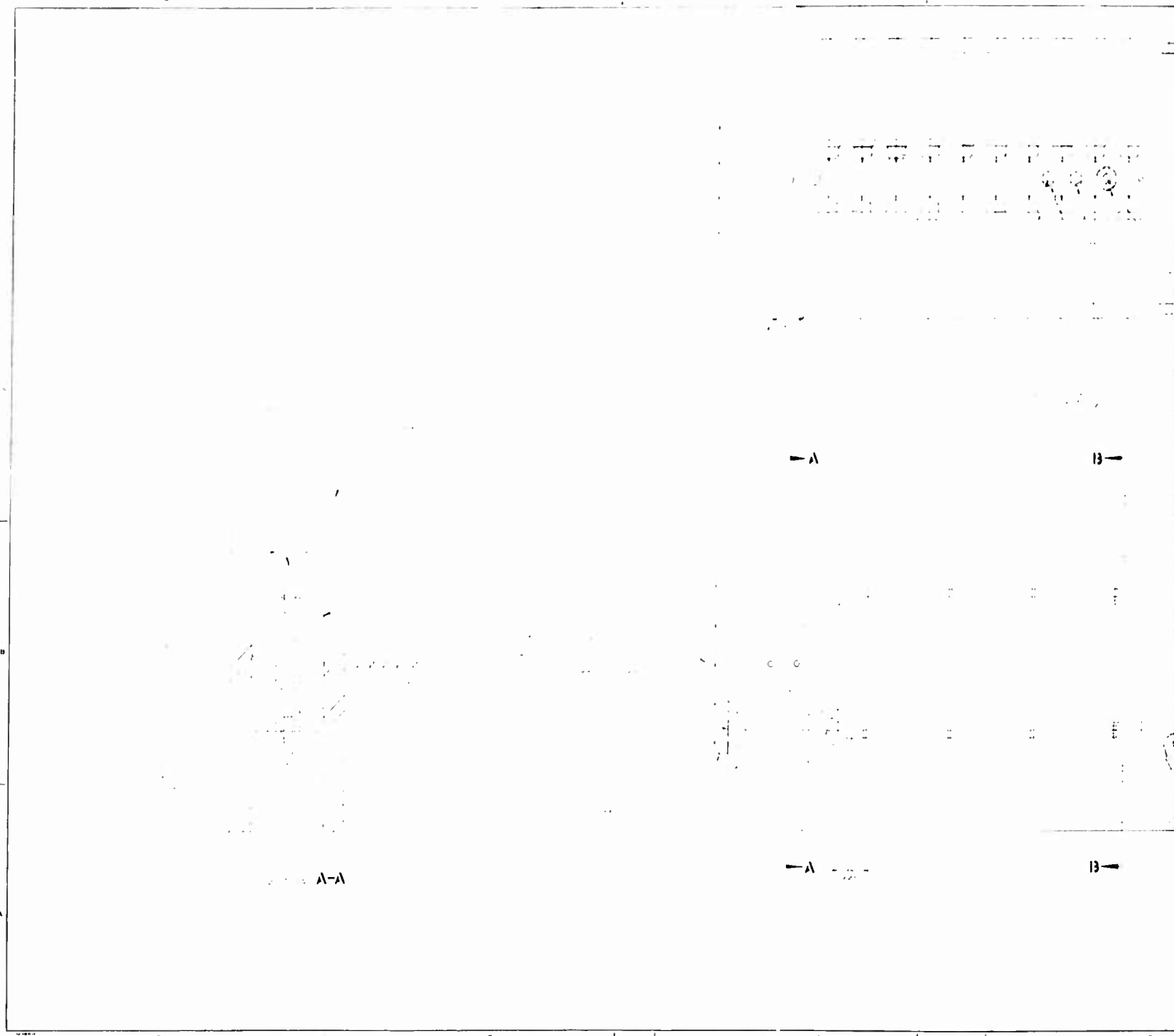
b. MAXIMUM COMBUSTION GAS VELOCITY
PROFILES FOR VARIOUS CHAMBER LENGTHS



c. INFINITE-WALL COMBUSTION
GAS VELOCITY PROFILE



d. WALL-EFFECT CORRELATION CURVES
FOR VARIOUS WIDTH CHAMBERS



1

13-

13-

13-13

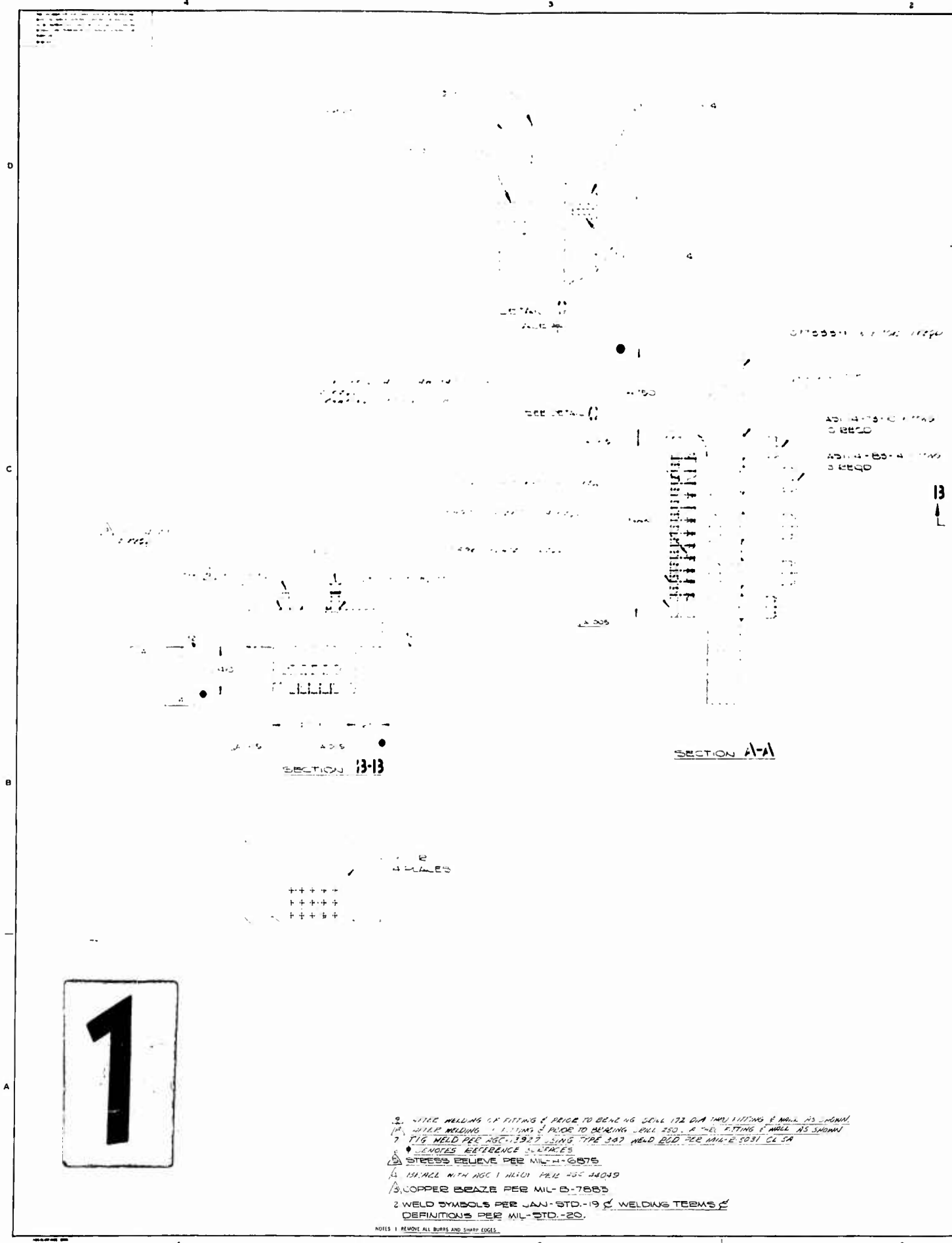
1. THEY WERE NOT KNOWN BEFORE WITHIN THE AREA OF THE
2. THIS WAS THE FIRST TIME IT WAS KNOWN
3. THE FIRST TIME IT WAS KNOWN
4. THE FIRST TIME IT WAS KNOWN
5. THE FIRST TIME IT WAS KNOWN
6. THE FIRST TIME IT WAS KNOWN
7. THE FIRST TIME IT WAS KNOWN
8. THE FIRST TIME IT WAS KNOWN
9. THE FIRST TIME IT WAS KNOWN
10. THE FIRST TIME IT WAS KNOWN

2

[illegible]

3

Figure 8



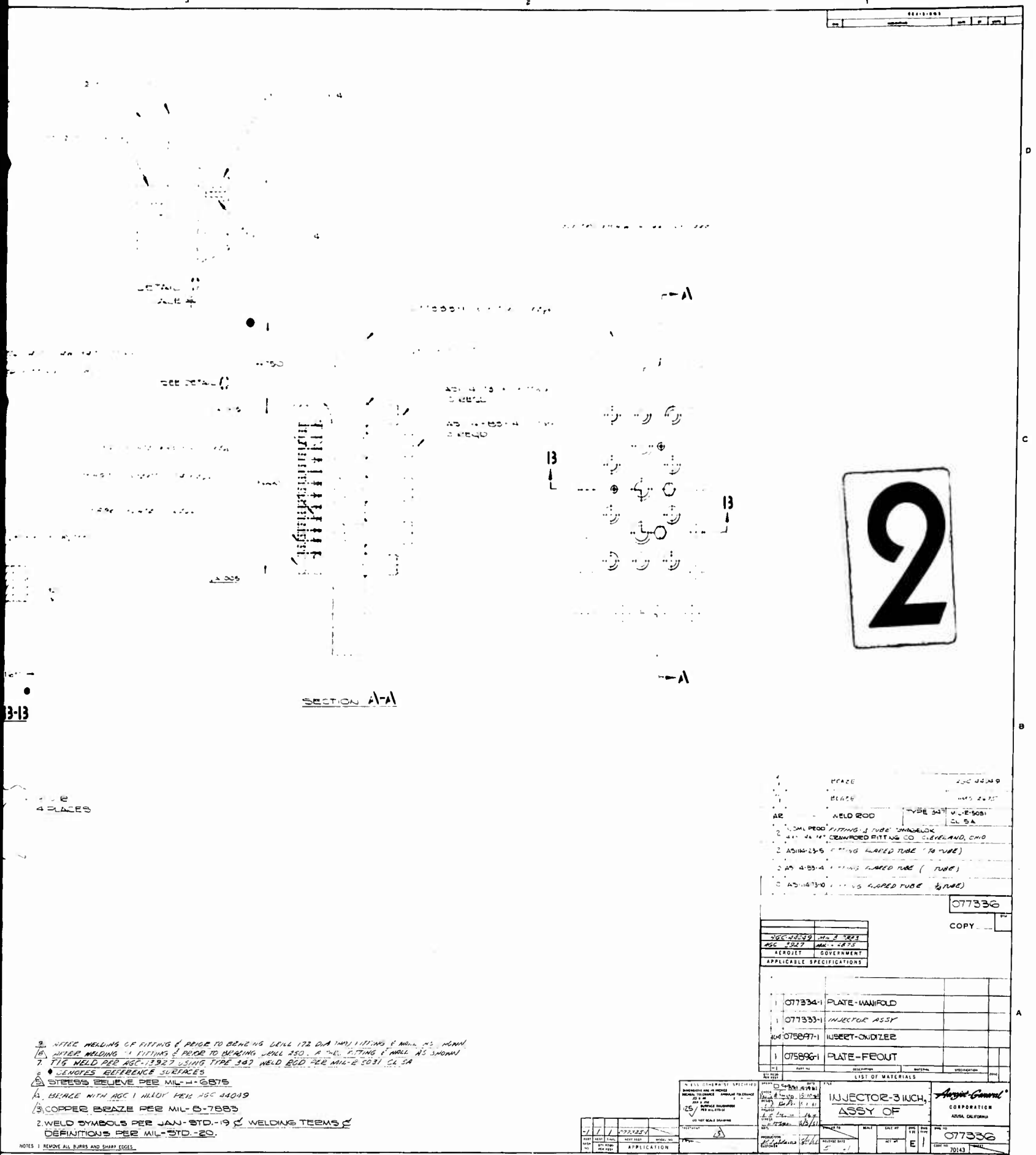


Figure 9

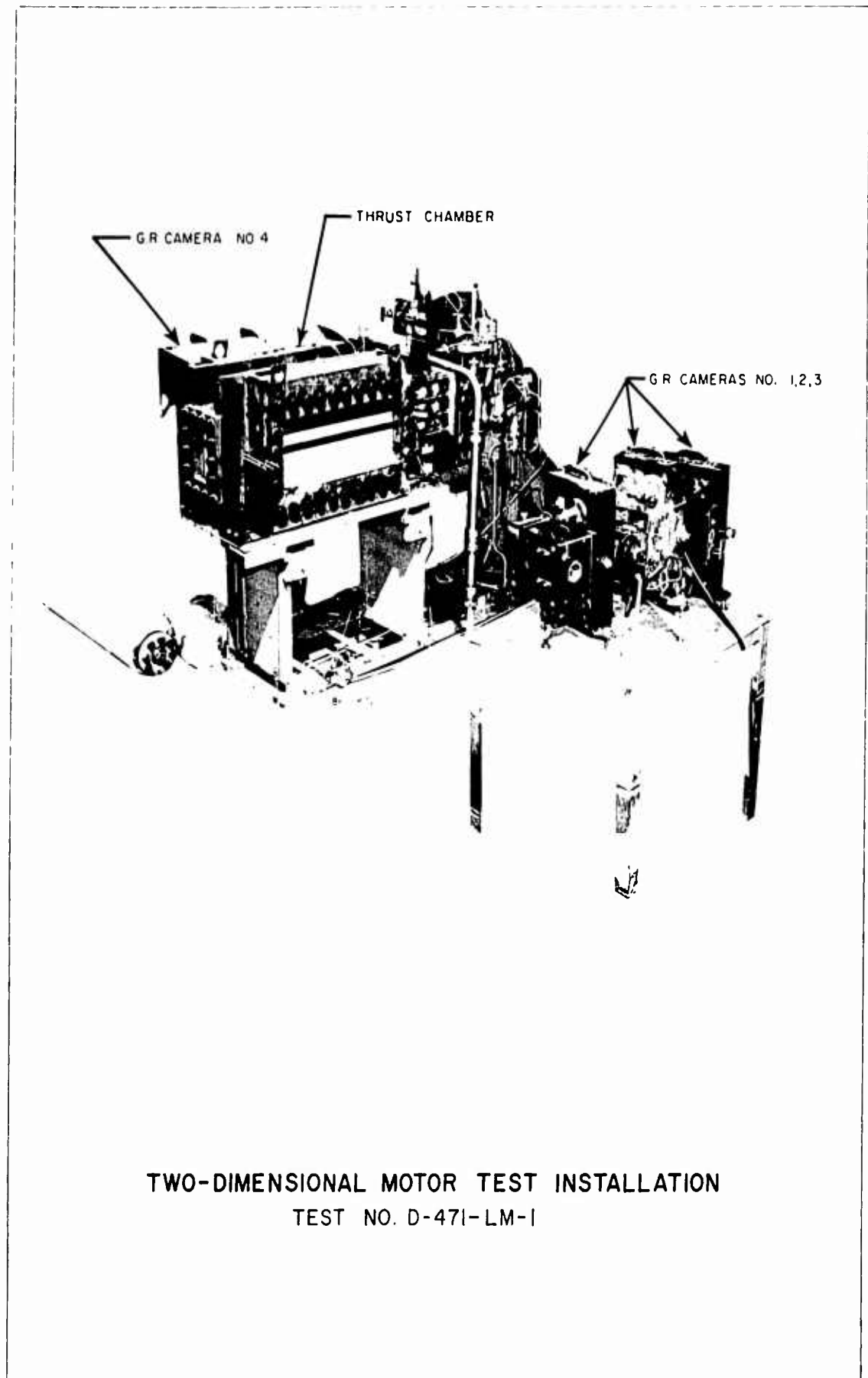
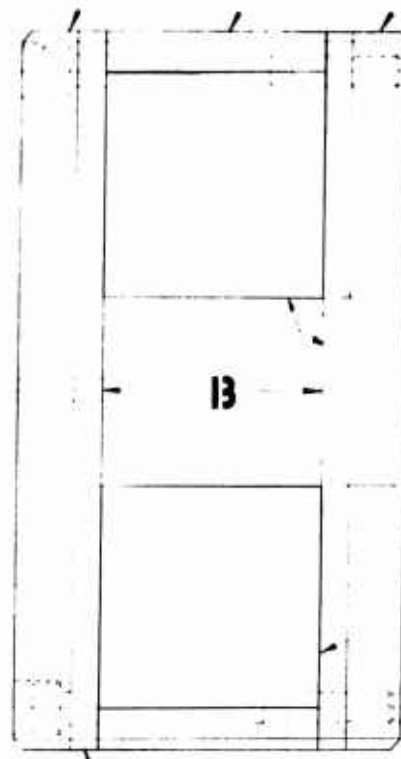
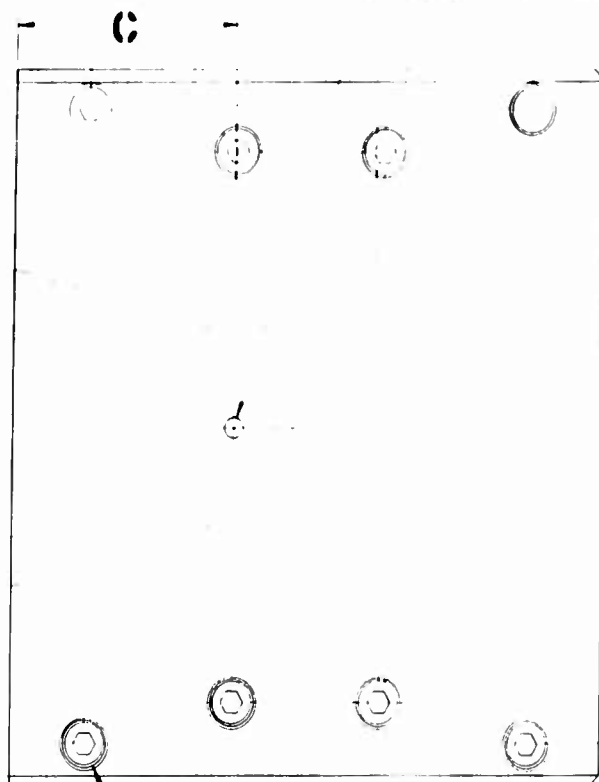


Figure 10

2054 NO ASSY	A	B	C
-1	3 12	1 00	1 400
-3	3 12	1 00	1 400
-5	4 38	50	4 900
-7	4 38	1 00	4 900
-9	2 21	1 00	2 320
-11	2 21	3 00	2 320

07735-1 LINER REQD ON -1, -5, -9 ASSY
07735-3 LINER REQD ON -3, -7, -11 ASSY

0754
0758
07732
07732
07732
07732



COML PROD 1/8-24 UNF-3A x 3.50 LG SLEN-
SOCKET HD 1/8 REQD ON -1, -5, -9 ASSY
COML PROD 1/8-24 UNF-3A x 4.50 LG SLEN-
SOCKET HD 1/8 REQD ON -3, -7, -11 ASSY
DUCOMMUN METALS & SUPPLY CO.

077346-1 LINER COPPER - 2 REQD

1

REFRACTORY COAT EXPOSED INSIDE SURFACES WITH
195 METAL #1 .005 IN. THICK.
2 RUBBER STAMP WITH PART NO. HERE.

NOTES: 1. REMOVE ALL BURRS AND SHARP EDGES

3

2

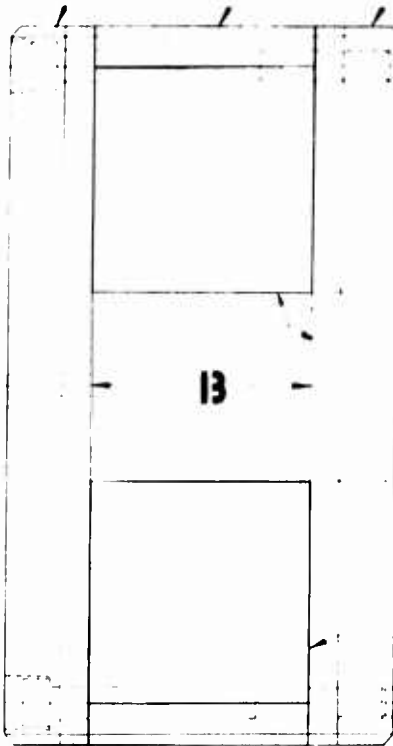
1

REVISIONS				
REV	DESCRIPTION	DATE	BY	APPROV

075894-1 NOZZLE - 2 LEVL ON - 1 ASSY
 075894-3 NOZZLE - 2 LEVL ON - 3 ASSY
 077327-1 NOZZLE - 2 LEVL ON - 5 ASSY
 077327-3 NOZZLE - 2 LEVL ON - 7 ASSY
 077332-1 NOZZLE - 2 LEVL ON - 9 ASSY
 077332-3 NOZZLE - 2 LEVL ON - 11 ASSY

20 ON - 15 2 ASSY
 20 ON - 15 11 ASSY

075894-1 LINER - 2 LEVL ON - 15 2 ASSY
 075894-3 LINER - 2 LEVL ON - 15 11 ASSY



A

NOTE: LINER - 2 LEVL ON - 15 2 ASSY
 LINER - 2 LEVL ON - 15 11 ASSY

077346-1 LINER - COPPER - 2 LEVL

2

REV	DESCRIPTION	DATE	BY	APPROV
1	NOZZLE - 2 LEVL ON - 1 ASSY			
2	NOZZLE - 2 LEVL ON - 3 ASSY			
3	NOZZLE - 2 LEVL ON - 5 ASSY			
4	NOZZLE - 2 LEVL ON - 7 ASSY			
5	NOZZLE - 2 LEVL ON - 9 ASSY			
6	NOZZLE - 2 LEVL ON - 11 ASSY			
7	NOZZLE - 2 LEVL ON - 13 ASSY			
8	NOZZLE - 2 LEVL ON - 15 ASSY			
9	NOZZLE - 2 LEVL ON - 17 ASSY			
10	NOZZLE - 2 LEVL ON - 19 ASSY			
11	NOZZLE - 2 LEVL ON - 21 ASSY			
12	NOZZLE - 2 LEVL ON - 23 ASSY			
13	NOZZLE - 2 LEVL ON - 25 ASSY			
14	NOZZLE - 2 LEVL ON - 27 ASSY			
15	NOZZLE - 2 LEVL ON - 29 ASSY			
16	NOZZLE - 2 LEVL ON - 31 ASSY			
17	NOZZLE - 2 LEVL ON - 33 ASSY			
18	NOZZLE - 2 LEVL ON - 35 ASSY			
19	NOZZLE - 2 LEVL ON - 37 ASSY			
20	NOZZLE - 2 LEVL ON - 39 ASSY			
21	NOZZLE - 2 LEVL ON - 41 ASSY			
22	NOZZLE - 2 LEVL ON - 43 ASSY			
23	NOZZLE - 2 LEVL ON - 45 ASSY			
24	NOZZLE - 2 LEVL ON - 47 ASSY			
25	NOZZLE - 2 LEVL ON - 49 ASSY			
26	NOZZLE - 2 LEVL ON - 51 ASSY			
27	NOZZLE - 2 LEVL ON - 53 ASSY			
28	NOZZLE - 2 LEVL ON - 55 ASSY			
29	NOZZLE - 2 LEVL ON - 57 ASSY			
30	NOZZLE - 2 LEVL ON - 59 ASSY			
31	NOZZLE - 2 LEVL ON - 61 ASSY			
32	NOZZLE - 2 LEVL ON - 63 ASSY			
33	NOZZLE - 2 LEVL ON - 65 ASSY			
34	NOZZLE - 2 LEVL ON - 67 ASSY			
35	NOZZLE - 2 LEVL ON - 69 ASSY			
36	NOZZLE - 2 LEVL ON - 71 ASSY			
37	NOZZLE - 2 LEVL ON - 73 ASSY			
38	NOZZLE - 2 LEVL ON - 75 ASSY			
39	NOZZLE - 2 LEVL ON - 77 ASSY			
40	NOZZLE - 2 LEVL ON - 79 ASSY			
41	NOZZLE - 2 LEVL ON - 81 ASSY			
42	NOZZLE - 2 LEVL ON - 83 ASSY			
43	NOZZLE - 2 LEVL ON - 85 ASSY			
44	NOZZLE - 2 LEVL ON - 87 ASSY			
45	NOZZLE - 2 LEVL ON - 89 ASSY			
46	NOZZLE - 2 LEVL ON - 91 ASSY			
47	NOZZLE - 2 LEVL ON - 93 ASSY			
48	NOZZLE - 2 LEVL ON - 95 ASSY			
49	NOZZLE - 2 LEVL ON - 97 ASSY			
50	NOZZLE - 2 LEVL ON - 99 ASSY			
51	NOZZLE - 2 LEVL ON - 101 ASSY			
52	NOZZLE - 2 LEVL ON - 103 ASSY			
53	NOZZLE - 2 LEVL ON - 105 ASSY			
54	NOZZLE - 2 LEVL ON - 107 ASSY			
55	NOZZLE - 2 LEVL ON - 109 ASSY			
56	NOZZLE - 2 LEVL ON - 111 ASSY			
57	NOZZLE - 2 LEVL ON - 113 ASSY			
58	NOZZLE - 2 LEVL ON - 115 ASSY			
59	NOZZLE - 2 LEVL ON - 117 ASSY			
60	NOZZLE - 2 LEVL ON - 119 ASSY			
61	NOZZLE - 2 LEVL ON - 121 ASSY			
62	NOZZLE - 2 LEVL ON - 123 ASSY			
63	NOZZLE - 2 LEVL ON - 125 ASSY			
64	NOZZLE - 2 LEVL ON - 127 ASSY			
65	NOZZLE - 2 LEVL ON - 129 ASSY			
66	NOZZLE - 2 LEVL ON - 131 ASSY			
67	NOZZLE - 2 LEVL ON - 133 ASSY			
68	NOZZLE - 2 LEVL ON - 135 ASSY			
69	NOZZLE - 2 LEVL ON - 137 ASSY			
70	NOZZLE - 2 LEVL ON - 139 ASSY			
71	NOZZLE - 2 LEVL ON - 141 ASSY			
72	NOZZLE - 2 LEVL ON - 143 ASSY			
73	NOZZLE - 2 LEVL ON - 145 ASSY			
74	NOZZLE - 2 LEVL ON - 147 ASSY			
75	NOZZLE - 2 LEVL ON - 149 ASSY			
76	NOZZLE - 2 LEVL ON - 151 ASSY			
77	NOZZLE - 2 LEVL ON - 153 ASSY			
78	NOZZLE - 2 LEVL ON - 155 ASSY			
79	NOZZLE - 2 LEVL ON - 157 ASSY			
80	NOZZLE - 2 LEVL ON - 159 ASSY			
81	NOZZLE - 2 LEVL ON - 161 ASSY			
82	NOZZLE - 2 LEVL ON - 163 ASSY			
83	NOZZLE - 2 LEVL ON - 165 ASSY			
84	NOZZLE - 2 LEVL ON - 167 ASSY			
85	NOZZLE - 2 LEVL ON - 169 ASSY			
86	NOZZLE - 2 LEVL ON - 171 ASSY			
87	NOZZLE - 2 LEVL ON - 173 ASSY			
88	NOZZLE - 2 LEVL ON - 175 ASSY			
89	NOZZLE - 2 LEVL ON - 177 ASSY			
90	NOZZLE - 2 LEVL ON - 179 ASSY			
91	NOZZLE - 2 LEVL ON - 181 ASSY			
92	NOZZLE - 2 LEVL ON - 183 ASSY			
93	NOZZLE - 2 LEVL ON - 185 ASSY			
94	NOZZLE - 2 LEVL ON - 187 ASSY			
95	NOZZLE - 2 LEVL ON - 189 ASSY			
96	NOZZLE - 2 LEVL ON - 191 ASSY			
97	NOZZLE - 2 LEVL ON - 193 ASSY			
98	NOZZLE - 2 LEVL ON - 195 ASSY			
99	NOZZLE - 2 LEVL ON - 197 ASSY			
100	NOZZLE - 2 LEVL ON - 199 ASSY			

077337	077337
COPY	
AEROJET	GOVERNMENT
APPLICABLE SPECIFICATIONS	

REV	DESCRIPTION	DATE	BY	APPROV
1	NOZZLE - 2 LEVL ON - 1 ASSY			
2	NOZZLE - 2 LEVL ON - 3 ASSY			
3	NOZZLE - 2 LEVL ON - 5 ASSY			
4	NOZZLE - 2 LEVL ON - 7 ASSY			
5	NOZZLE - 2 LEVL ON - 9 ASSY			
6	NOZZLE - 2 LEVL ON - 11 ASSY			
7	NOZZLE - 2 LEVL ON - 13 ASSY			
8	NOZZLE - 2 LEVL ON - 15 ASSY			
9	NOZZLE - 2 LEVL ON - 17 ASSY			
10	NOZZLE - 2 LEVL ON - 19 ASSY			
11	NOZZLE - 2 LEVL ON - 21 ASSY			
12	NOZZLE - 2 LEVL ON - 23 ASSY			
13	NOZZLE - 2 LEVL ON - 25 ASSY			
14	NOZZLE - 2 LEVL ON - 27 ASSY			
15	NOZZLE - 2 LEVL ON - 29 ASSY			
16	NOZZLE - 2 LEVL ON - 31 ASSY			
17	NOZZLE - 2 LEVL ON - 33 ASSY			
18	NOZZLE - 2 LEVL ON - 35 ASSY			
19	NOZZLE - 2 LEVL ON - 37 ASSY			
20	NOZZLE - 2 LEVL ON - 39 ASSY			
21	NOZZLE - 2 LEVL ON - 41 ASSY			
22	NOZZLE - 2 LEVL ON - 43 ASSY			
23	NOZZLE - 2 LEVL ON - 45 ASSY			
24	NOZZLE - 2 LEVL ON - 47 ASSY			
25	NOZZLE - 2 LEVL ON - 49 ASSY			
26	NOZZLE - 2 LEVL ON - 51 ASSY			
27	NOZZLE - 2 LEVL ON - 53 ASSY			
28	NOZZLE - 2 LEVL ON - 55 ASSY			
29	NOZZLE - 2 LEVL ON - 57 ASSY			
30	NOZZLE - 2 LEVL ON - 59 ASSY			
31	NOZZLE - 2 LEVL ON - 61 ASSY			
32	NOZZLE - 2 LEVL ON - 63 ASSY			
33	NOZZLE - 2 LEVL ON - 65 ASSY			
34	NOZZLE - 2 LEVL ON - 67 ASSY			
35	NOZZLE - 2 LEVL ON - 69 ASSY			
36	NOZZLE - 2 LEVL ON - 71 ASSY			
37	NOZZLE - 2 LEVL ON - 73 ASSY			
38	NOZZLE - 2 LEVL ON - 75 ASSY			
39	NOZZLE - 2 LEVL ON - 77 ASSY			
40	NOZZLE - 2 LEVL ON - 79 ASSY			
41	NOZZLE - 2 LEVL ON - 81 ASSY			
42	NOZZLE - 2 LEVL ON - 83 ASSY			
43	NOZZLE - 2 LEVL ON - 85 ASSY			
44	NOZZLE - 2 LEVL ON - 87 ASSY			
45	NOZZLE - 2 LEVL ON - 89 ASSY			
46	NOZZLE - 2 LEVL ON - 91 ASSY			
47	NOZZLE - 2 LEVL ON - 93 ASSY			
48	NOZZLE - 2 LEVL ON - 95 ASSY			
49	NOZZLE - 2 LEVL ON - 97 ASSY			
50	NOZZLE - 2 LEVL ON - 99 ASSY			
51	NOZZLE - 2 LEVL ON - 101 ASSY			
52	NOZZLE - 2 LEVL ON - 103 ASSY			
53	NOZZLE - 2 LEVL ON - 105 ASSY			
54	NOZZLE - 2 LEVL ON - 107 ASSY			
55	NOZZLE - 2 LEVL ON - 109 ASSY			
56	NOZZLE - 2 LEVL ON - 111 ASSY			
57	NOZZLE - 2 LEVL ON - 113 ASSY			
58	NOZZLE - 2 LEVL ON - 115 ASSY			
59	NOZZLE - 2 LEVL ON - 117 ASSY			
60	NOZZLE - 2 LEVL ON - 119 ASSY			
61	NOZZLE - 2 LEVL ON - 121 ASSY			
62	NOZZLE - 2 LEVL ON - 123 ASSY			
63	NOZZLE - 2 LEVL ON - 125 ASSY			
64	NOZZLE - 2 LEVL ON - 127 ASSY			
65	NOZZLE - 2 LEVL ON - 129 ASSY			
66	NOZZLE - 2 LEVL ON - 131 ASSY			
67	NOZZLE - 2 LEVL ON - 133 ASSY			
68	NOZZLE - 2 LEVL ON - 135 ASSY			
69	NOZZLE - 2 LEVL ON - 137 ASSY			
70	NOZZLE - 2 LEVL ON - 139 ASSY			
71	NOZZLE - 2 LEVL ON - 141 ASSY			
72	NOZZLE - 2 LEVL ON - 143 ASSY			
73	NOZZLE - 2 LEVL ON - 145 ASSY			
74	NOZZLE - 2 LEVL ON - 147 ASSY			
75	NOZZLE - 2 LEVL ON - 149 ASSY			
76	NOZZLE - 2 LEVL ON - 151 ASSY			
77	NOZZLE - 2 LEVL ON - 153 ASSY			
78	NOZZLE - 2 LEVL ON - 155 ASSY			
79	NOZZLE - 2 LEVL ON - 157 ASSY			
80	NOZZLE - 2 LEVL ON - 159 ASSY			
81	NOZZLE - 2 LEVL ON - 161 ASSY			
82	NOZZLE - 2 LEVL ON - 163 ASSY			
83	NOZZLE - 2 LEVL ON - 165 ASSY			
84	NOZZLE - 2 LEVL ON - 167 ASSY			
85	NOZZLE - 2 LEVL ON - 169 ASSY			
86	NOZZLE - 2 LEVL ON - 171 ASSY			
87	NOZZLE - 2 LEVL ON - 173 ASSY			
88	NOZZLE - 2 LEVL ON - 175 ASSY			
89	NOZZLE - 2 LEVL ON - 177 ASSY			
90	NOZZLE - 2 LEVL ON - 179 ASSY			
91	NOZZLE - 2 LEVL ON - 181 ASSY			
92	NOZZLE - 2 LEVL ON - 183 ASSY			
93	NOZZLE - 2 LEVL ON - 185 ASSY			
94	NOZZLE - 2 LEVL ON - 187 ASSY			
95	NOZZLE - 2 LEVL ON - 189 ASSY			
96	NOZZLE - 2 LEVL ON - 191 ASSY			
97	NOZZLE - 2 LEVL ON - 193 ASSY			
98	NOZZLE - 2 LEVL ON - 195 ASSY			
99	NOZZLE - 2 LEVL ON - 197 ASSY			
100	NOZZLE - 2 LEVL ON - 199 ASSY			

UNLESS OTHERWISE SPECIFIED		DRAWN BY: J. E. G. 10/10/61		CHECKED BY: J. E. G. 10/10/61		APPROVED BY: J. E. G. 10/10/61	
DIMENSIONS ARE IN INCHES		SCALE: 1/2" = 1"		MATERIAL: COPPER		SPECIFICATION: 077337	
TOLERANCES: .005" MAX		FINISH: 100		TREATMENT: 100		APPROVAL: 100	
DO NOT SCALE DRAWING		RELEASE DATE: 10/10/61		SCALE: 1/2" = 1"		ACT. WT: D 1	
PART NAME: NOZZLE ASSY-CHAMBER		SCALE: 1/2" = 1"		ACT. WT: D 1		DOW NO. 077337	
PART NO. 077337		SCALE: 1/2" = 1"		ACT. WT: D 1		CODE IDENT NO. 70143	
PART NO. 077337		SCALE: 1/2" = 1"		ACT. WT: D 1		CODE IDENT NO. 70143	

Figure 11

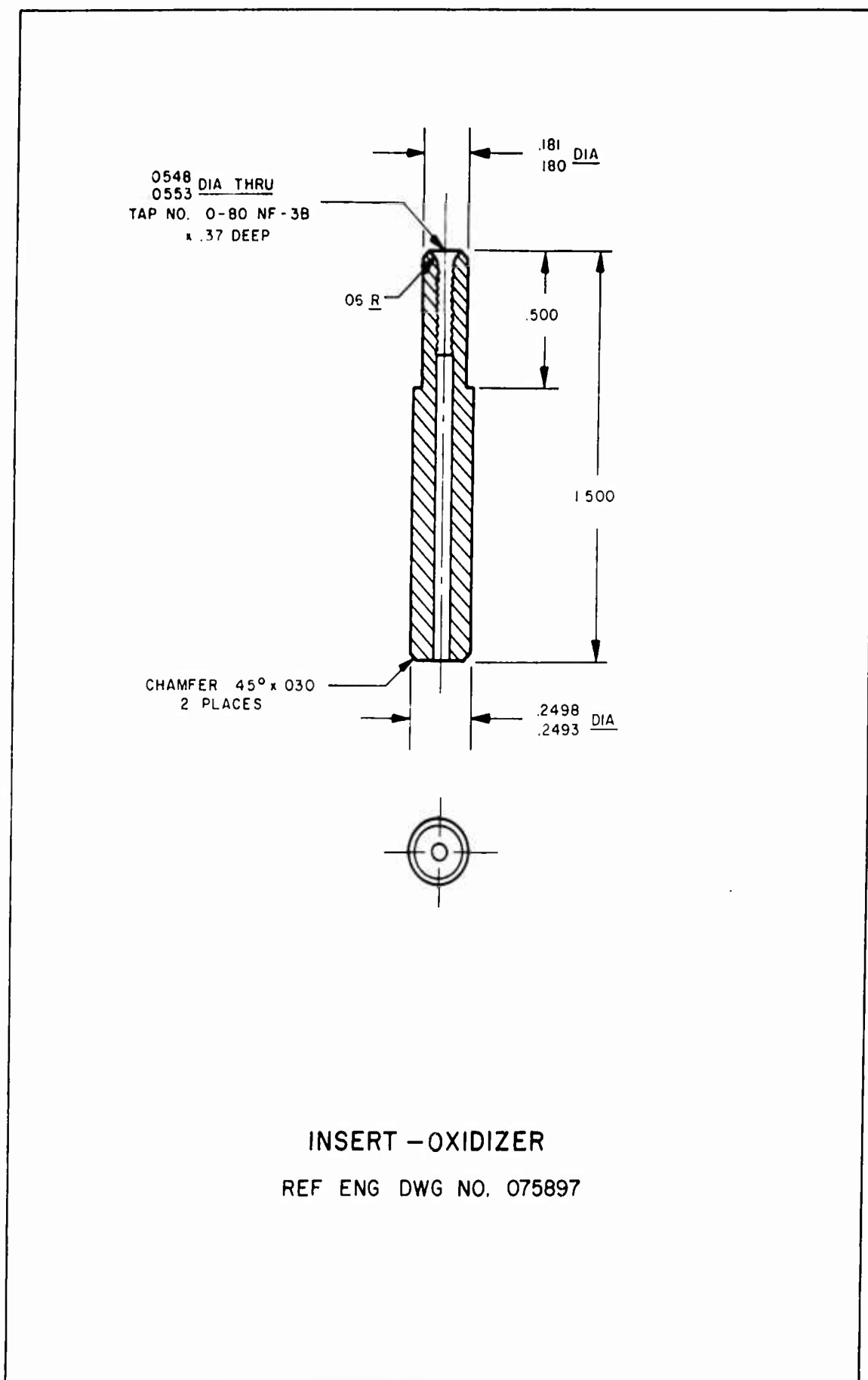
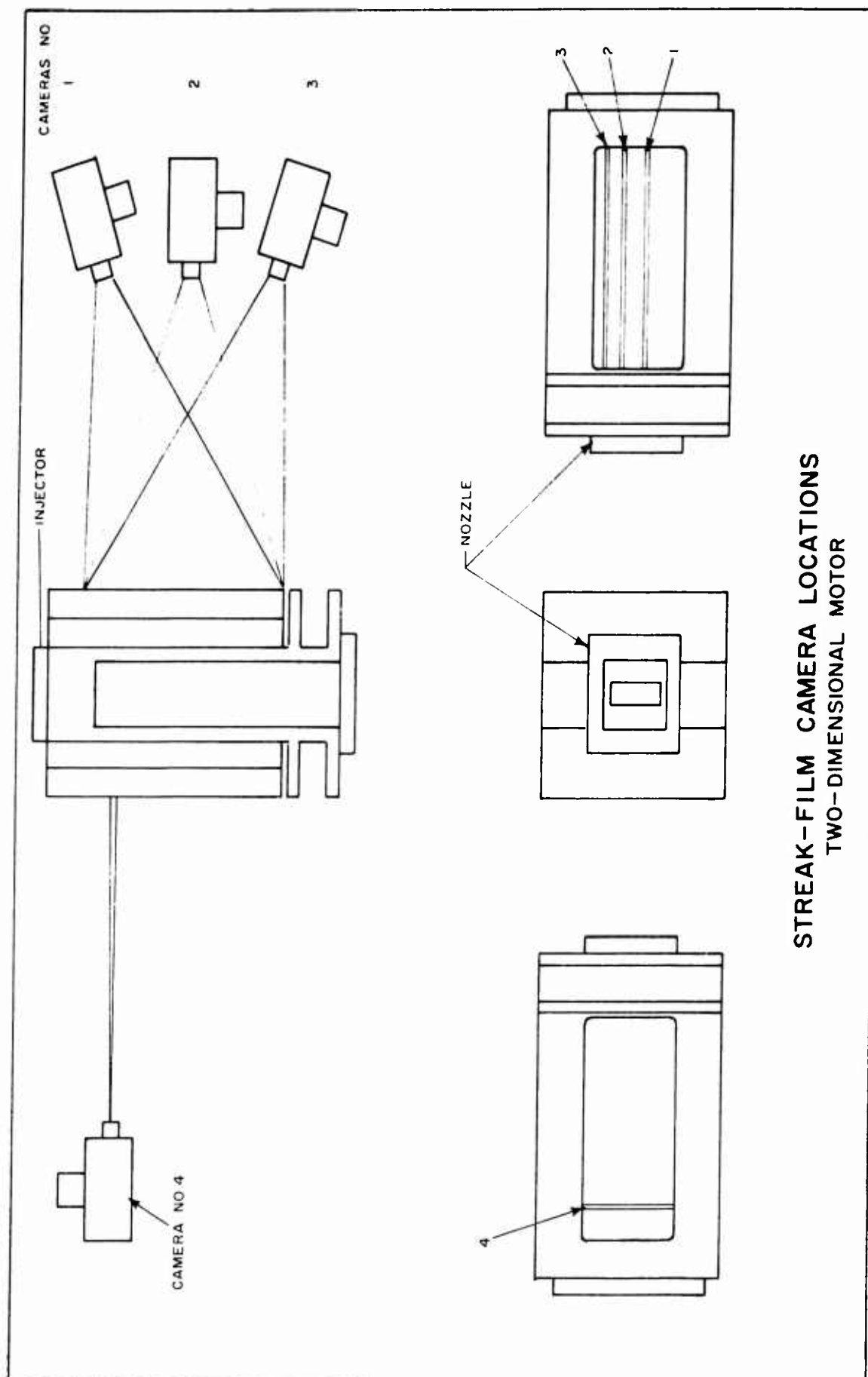


Figure 12



STREAK-FILM CAMERA LOCATIONS
TWO-DIMENSIONAL MOTOR

Figure 13

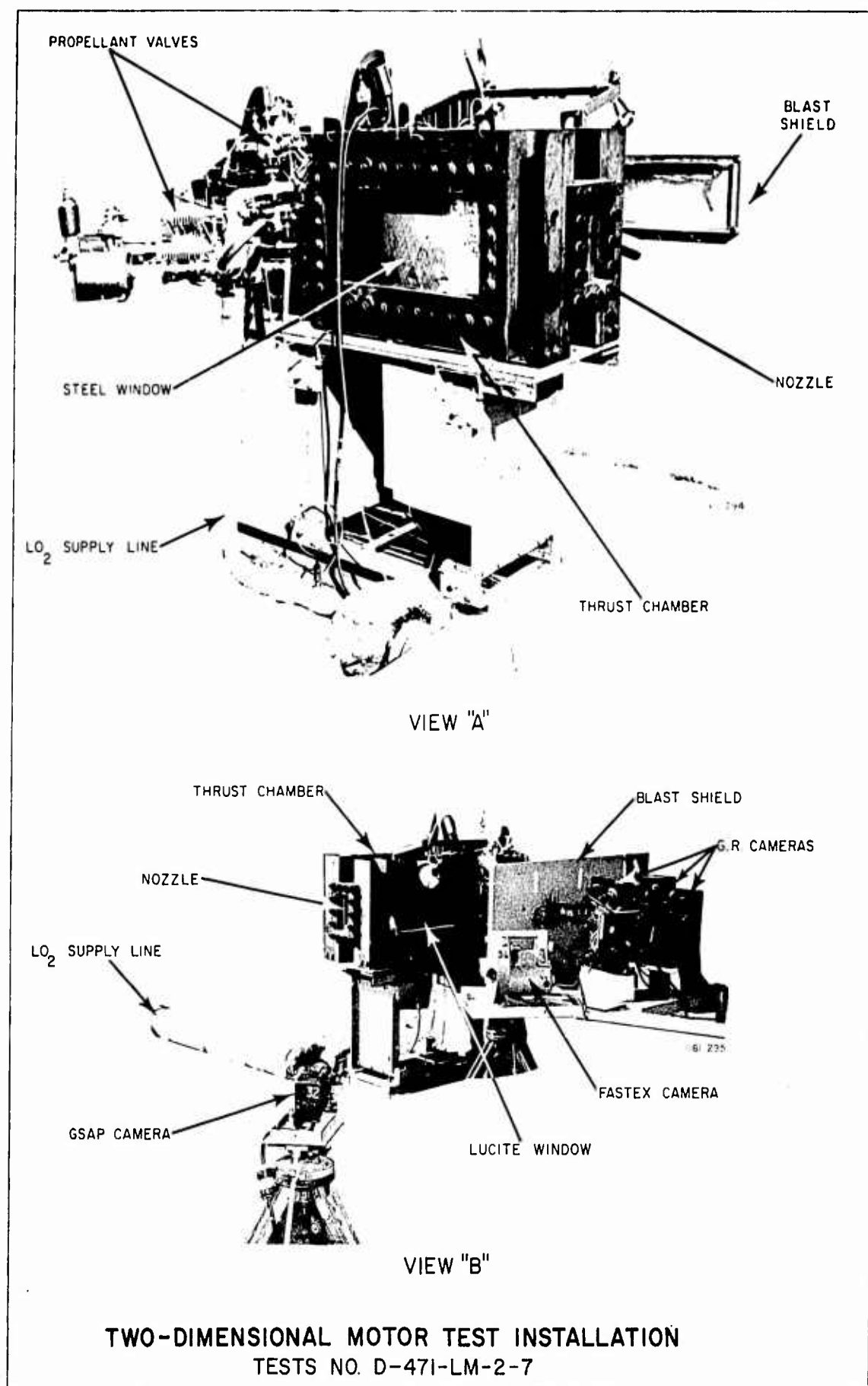


Figure 14

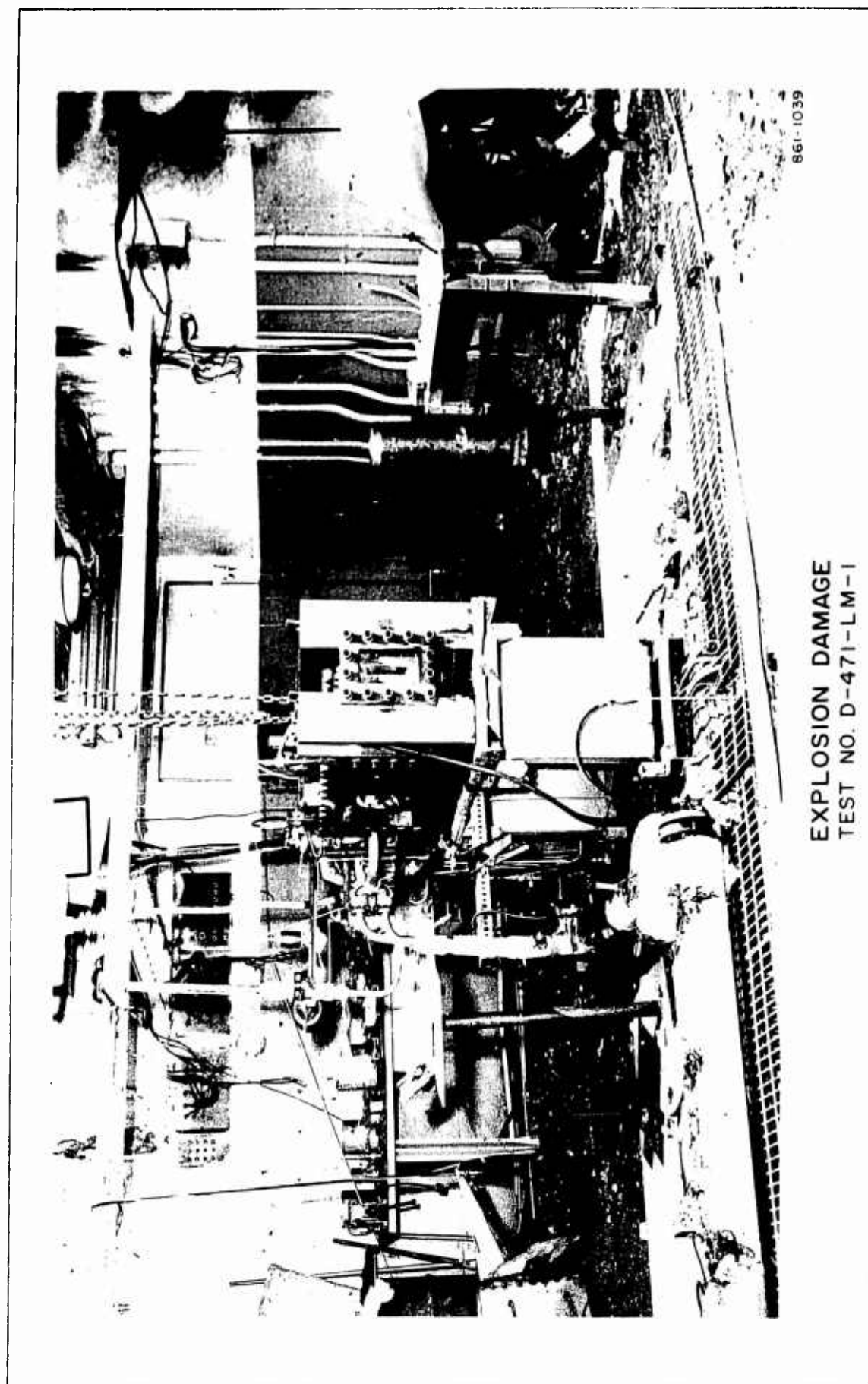


Figure 15

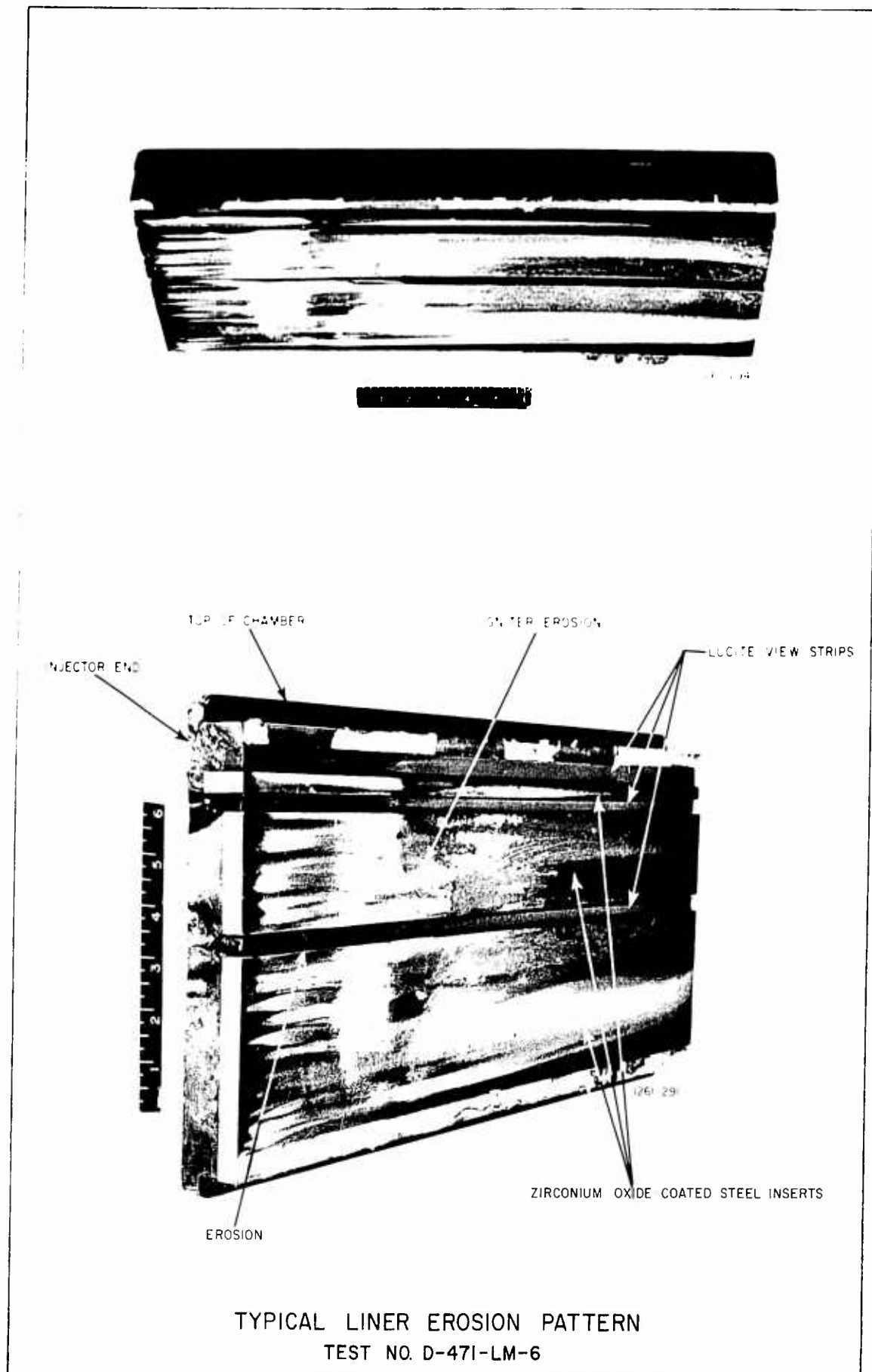
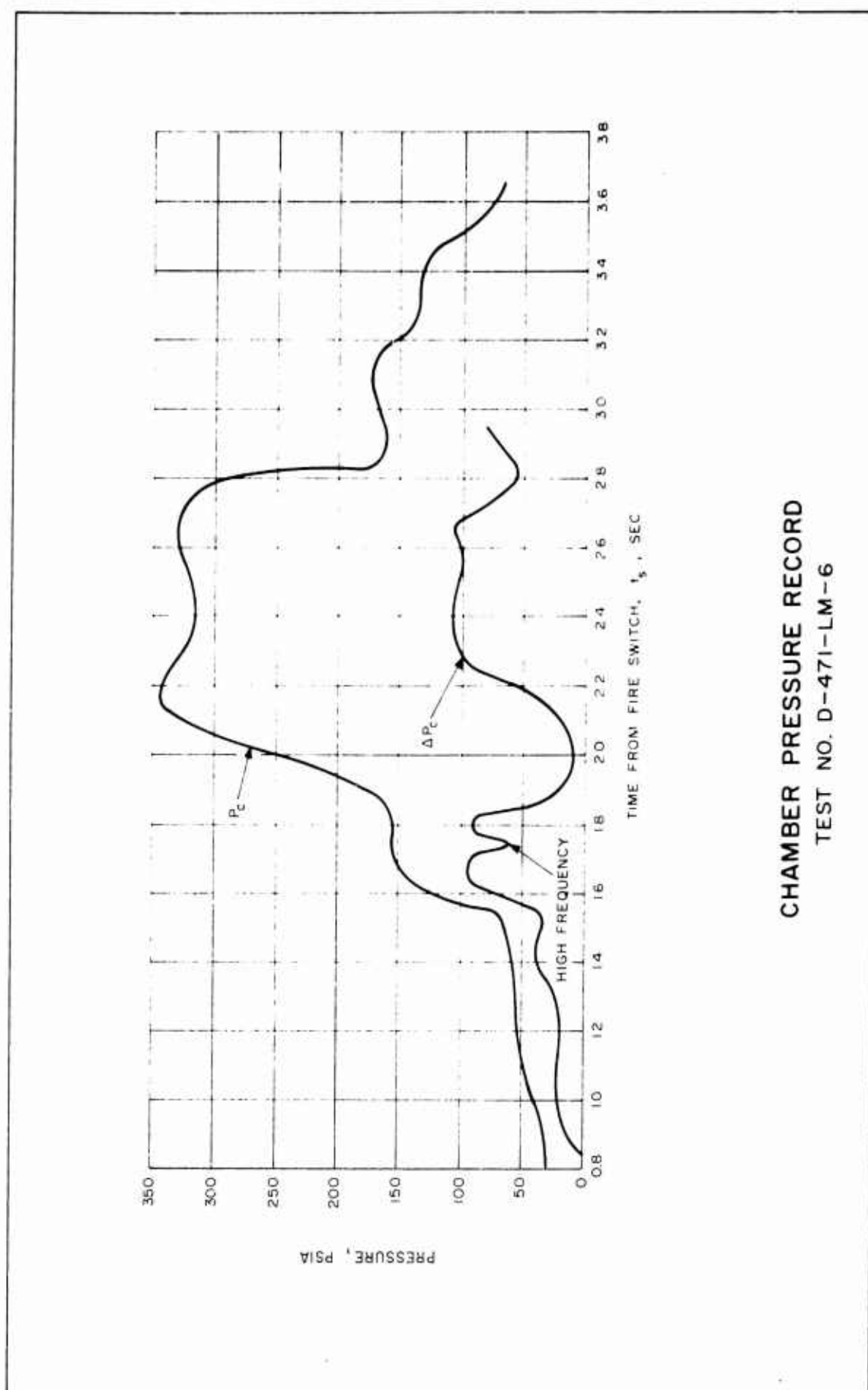
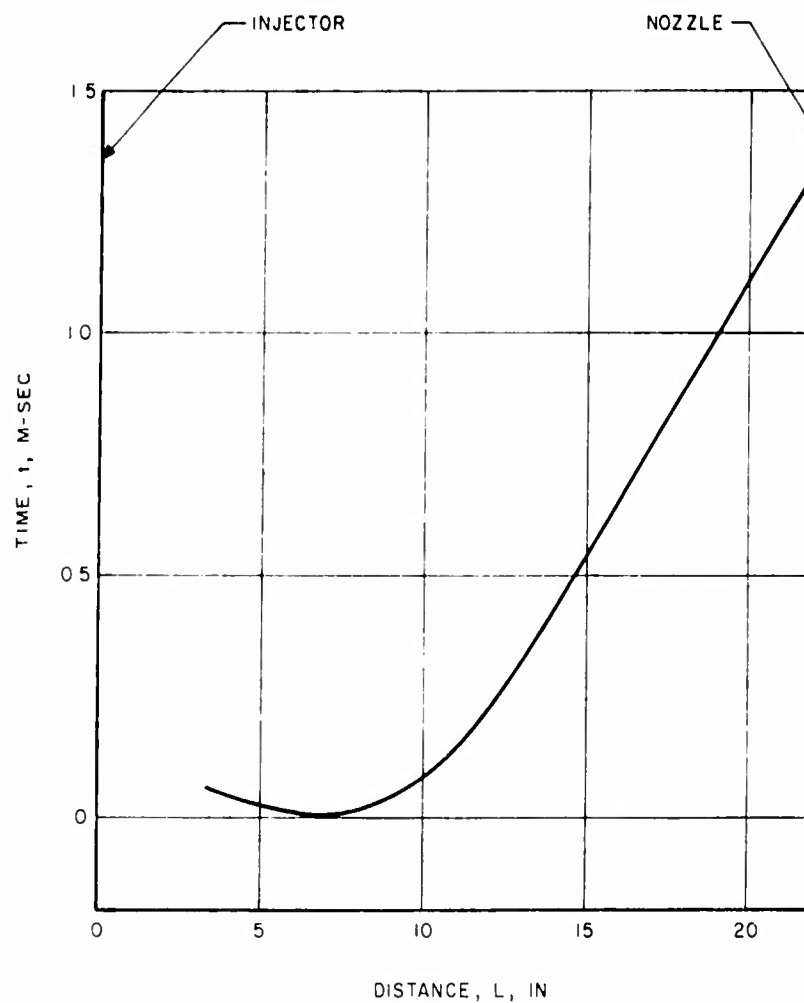


Figure 16



CHAMBER PRESSURE RECORD
TEST NO. D-471-LM-6

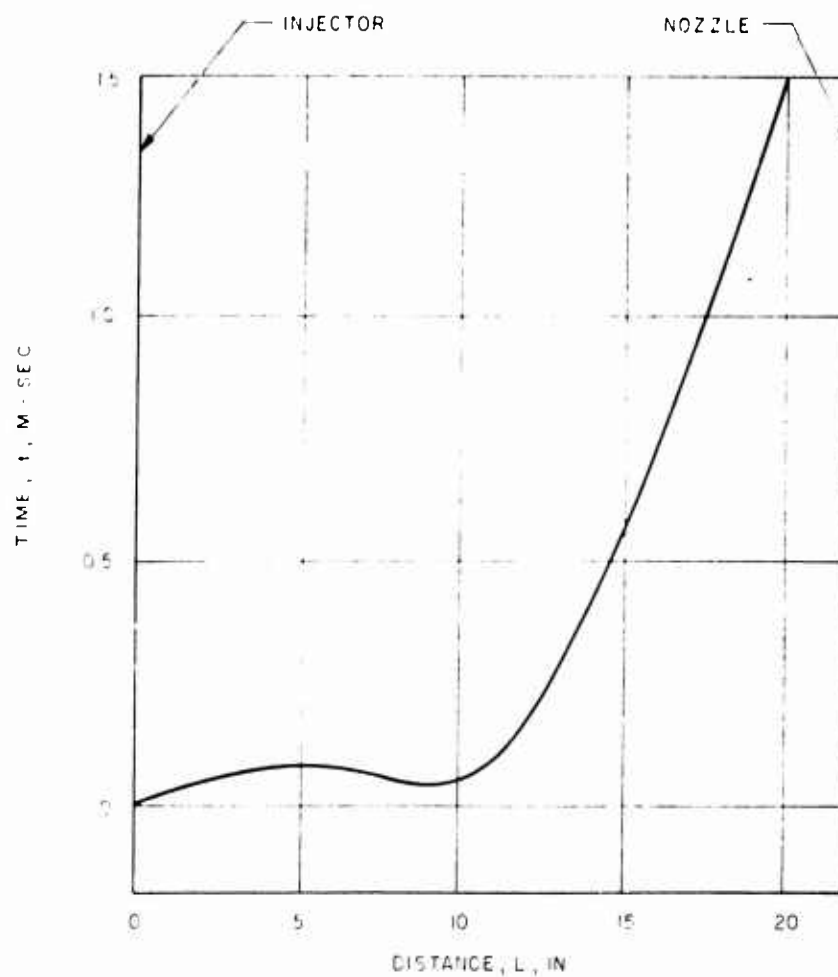
Figure 17



$P_c = 62 \text{ psia}$
 $\dot{W}_p = 3.5 \text{ lbs/sec}$
 $M.R. = 1.5$

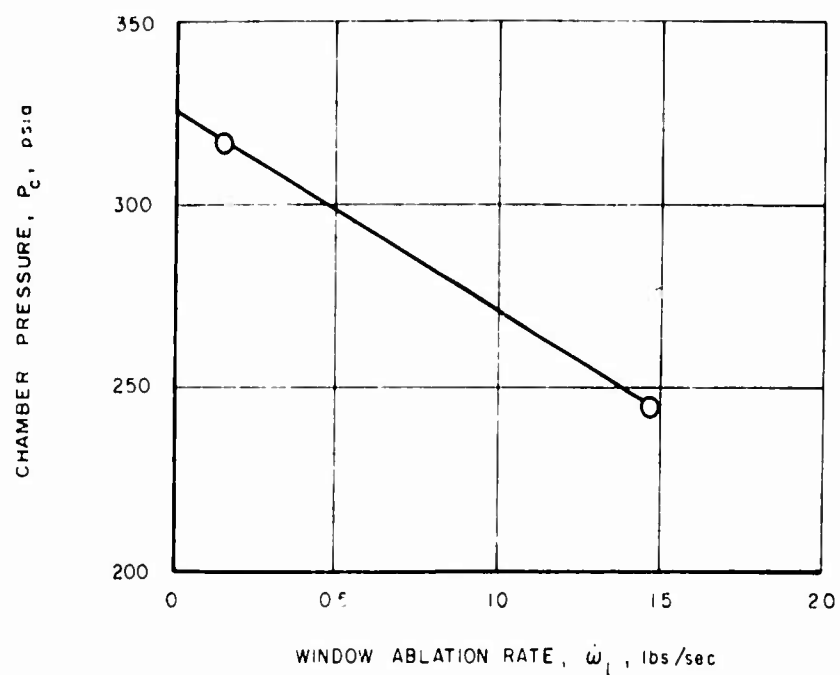
GASEOUS PARTICLE MOTION
TEST NO. D-471-LM-3
CAMERA NO. 2

Figure 18

 $P_c = 217 \text{ psia}$ $W_p = 7.6 \text{ lbs/sec}$ $M.R. = 1.5$

GASEOUS PARTICLE MOTION
TEST NO. D-471-LM-7
CAMERA NO. 2

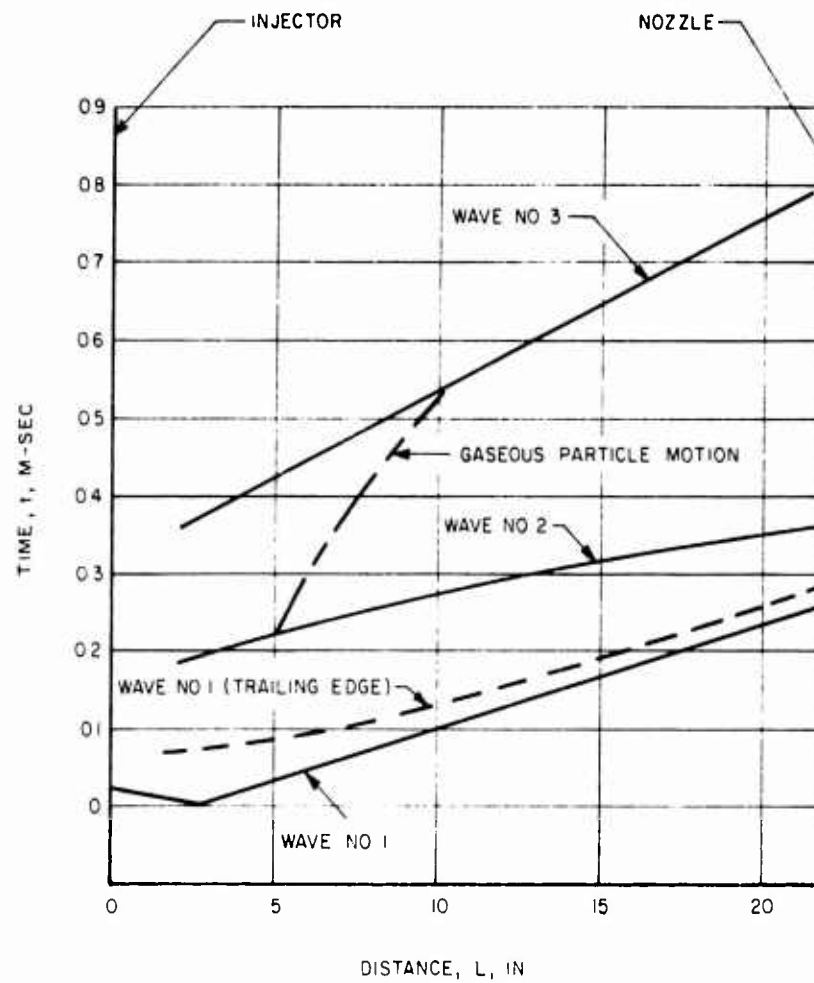
Figure 19



TEST NO.	$\dot{\omega}_p$	$\dot{\omega}_L$	P_c	η
-4	5.77	1.47	245	70.2
-6	6.02	0.15	317	86.1
EST.	—	0	323	88.3

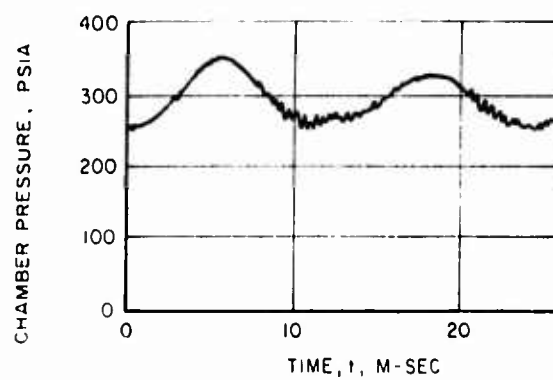
EFFECT OF LUCITE ABLATION ON COMBUSTION EFFICIENCY

TESTS NO. D-471-LM-4, 6



DETONATION WAVES
TEST NO. D-471-LM-1
CAMERA NO. 2

Figure 21

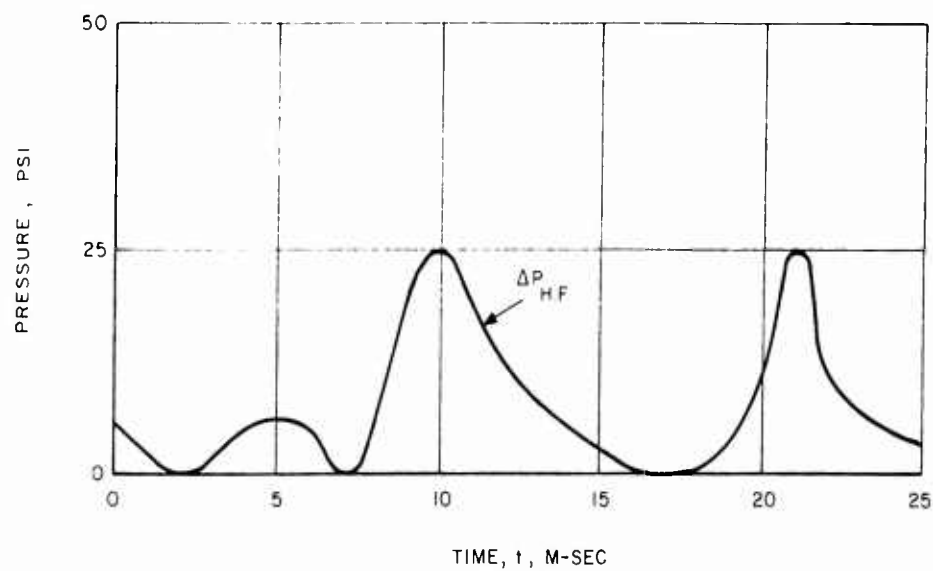


$$\Delta P_{HF} = 25 \text{ psi}$$

$$f_{HF} = 2300 \text{ cps}$$

$$\Delta P_{LF} = 100 \text{ psi}$$

$$f_{LF} = 77 \text{ cps}$$



$$P_c = 315 \text{ psia}$$

$$\dot{W}_p = 6.0 \text{ lb/sec}$$

$$M.R. = 2.2$$

$$t_s = 2.369 \text{ SEC FROM FIRE SWITCH}$$

COMBINED INSTABILITY
TEST NO. D-471-LM-6

Figure 22

TABLE 1
TWO-DIMENSIONAL MOTOR TESTS AND EXPERIMENTAL RESULTS

Test No.	Injector No.	Contraction Ratio	Chamber Width in.	Propellant	Chamber Pressure psia		Fuel Flow Rate lb/sec		Oxidizer Flow Rate lb/sec		Mixture Ratio		Combustion Efficiency %	Remarks
					Planned	Actual	Planned	Actual	Planned	Actual	Planned	Actual		
D-471-LM-1	077336-3	2.46	1.0	LO ₂ /RP-1	555	-	1.36	-	4.16	-	2.24	-	-	Explosion due to igniter position and propellant accumulation
2	077336-1 (modified)	2.46	1.0	LO ₂ /RP-1	-	-	1.36	-	4.16	-	2.24	-	-	Start-transient evaluation test
3	077336-1 (modified)	2.46	1.0	LO ₂ /RP-1	555	94	1.36	3.36	4.16	2.12	2.24	0.55	42.5	Improper metering devices
4	077336-1 (modified)	2.46	1.0	LO ₂ /RP-1	555	245	1.36	1.92	4.16	3.65	2.24	2.00	70.2	- - -
5	077336-1 (modified)	2.46	1.0	LO ₂ /RP-1	500	-	2.01	-	5.56	-	2.24	-	-	Explosion due to short in igniter circuit
6	077336-1 (modified)	2.46	1.0	LO ₂ /RP-1	555	517	1.36	1.00	4.16	4.13	2.24	2.19	86.1	- - -
7	077336-1 (modified)	2.46	1.0	LO ₂ /RP-1	500	431	2.01	2.02	5.56	5.90	2.24	2.25	82.5	Leak around nozzle closure

Table 1